


# Expression of Truncated Products at the 5'-Terminal Region of *RIPK2* and Evolutive Aspects that Support Their Biological Importance

Ulises M.M. Villagra<sup>1,†</sup>, Bianca R. da Cunha<sup>2,3,†</sup>, Giovana M. Polachini<sup>2,†</sup>, Tiago Henrique<sup>2</sup>, Ana Carolina Buzzo Stefanini<sup>3</sup>, Tialfi Bergamin de Castro<sup>2,4</sup>, Carlos H.T.P. da Silva<sup>5</sup>, Olavo A. Feitosa<sup>5</sup>, Erica E. Fukuyama<sup>6</sup>, Rossana V.M. López<sup>7</sup>, Emmanuel Dias-Neto<sup>8</sup>, Fabio D. Nunes<sup>9</sup>, Patricia Severino<sup>3,10</sup>, and Eloiza H. Tajara <sup>2,3,\*</sup>

<sup>1</sup>Faculty of Exact Sciences, Biotechnology and Molecular Biology Institute (IBBM), National University of La Plata-CCT, CONICET, La Plata, Argentina

<sup>2</sup>Department of Molecular Biology, School of Medicine of São José do Rio Preto/FAMERP, São José do Rio Preto, SP, Brazil

<sup>3</sup>Department of Genetics and Evolutionary Biology, Institute of Biosciences, University of São Paulo/USP, São Paulo, SP, Brazil

<sup>4</sup>Microbial Pathogenesis Department, University of Maryland Baltimore, School of Dentistry, Baltimore, MD, USA

<sup>5</sup>Computational Laboratory of Pharmaceutical Chemistry, School of Pharmaceutical Sciences of Ribeirão Preto, University of São Paulo/USP, Ribeirão Preto, SP, Brazil

<sup>6</sup>Head and Neck Surgery Department, Arnaldo Vieira de Carvalho Cancer Institute, São Paulo, SP, Brazil

<sup>7</sup>Comprehensive Center for Precision Oncology, Center for Translational Research in Oncology, State of São Paulo Cancer Institute—ICESP, Clinics Hospital, São Paulo University Medical School, São Paulo, SP, Brazil

<sup>8</sup>Laboratory of Medical Genomics, A.C. Camargo Cancer Center, São Paulo, SP, Brazil

<sup>9</sup>Department of Stomatology, School of Dentistry, University of São Paulo/USP, São Paulo, SP, Brazil

<sup>10</sup>Albert Einstein Research and Education Institute, Hospital Israelita Albert Einstein, São Paulo, SP, Brazil

<sup>†</sup>These authors contributed equally to this work.

\*Corresponding author: E-mail: [tajara@famerp.br](mailto:tajara@famerp.br).

Accepted: May 10, 2024

## Abstract

Alternative splicing is the process of generating different mRNAs from the same primary transcript, which contributes to increase the transcriptome and proteome diversity. Abnormal splicing has been associated with the development of several diseases including cancer. Given that mutations and abnormal levels of the RIPK2 transcript and RIP-2 protein are frequent in tumors, and that RIP-2 modulates immune and inflammatory responses, we investigated alternative splicing events that result in partial deletions of the kinase domain at the N-terminus of RIP-2. We also investigated the structure and expression of the RIPK2 truncated variants and isoforms in different environments. In addition, we searched data throughout Supraprimates evolution that could support the biological importance of RIPK2 alternatively spliced products. We observed that human variants and isoforms were differentially regulated following temperature stress, and that the truncated transcript was more expressed than the long transcript in tumor samples. The inverse was found for the longer protein isoform. The truncated variant was also detected in chimpanzee, gorilla, hare, pika, mouse, rat, and tree shrew. The fact that the same variant has been preserved in mammals with divergence times up to 70 million years raises the hypothesis that it may have a functional significance.

**Key words:** alternative splicing, RIPK2, RIP-2, gene expression, stress conditions, isoform conservation.

© The Author(s) 2024. Published by Oxford University Press on behalf of Society for Molecular Biology and Evolution.

This is an Open Access article distributed under the terms of the Creative Commons Attribution-NonCommercial License (<https://creativecommons.org/licenses/by-nc/4.0/>), which permits non-commercial re-use, distribution, and reproduction in any medium, provided the original work is properly cited. For commercial re-use, please contact [reprints@oup.com](mailto:reprints@oup.com) for reprints and translation rights for reprints. All other permissions can be obtained through our RightsLink service via the Permissions link on the article page on our site—for further information please contact [journals.permissions@oup.com](mailto:journals.permissions@oup.com).

## Significance

RIP-2 protein is a kinase that integrates extra- and intracellular stress signals and has an important role in modulating immune responses. *RIPK2* gene generates two transcripts by alternative splicing: the longest variant 1 encodes the canonical protein and the short variant 2 results in a predicted truncated product with a partially deleted kinase domain. In the present study, we observed that both transcripts were expressed in normal tissues, but differentially expressed in tumor samples and in response to temperature stress. The truncated variant is conserved in primates, hare, pika, mice, rats, and tree shrew, which diverged several million years ago. These findings suggest that this variant should have a biological role and stimulate further functional investigation.

## Introduction

Alternative splicing (AS) is an important and prevalent process in eukaryotic genes that generates different mature mRNA variants and protein isoforms from the same primary transcript. The patterns of AS comprise exon inclusion or skipping, unusual splice site selection and intron retention, which can result in an alternative translation initiation site (TIS) or in premature termination codons (Park, et al. 2018). Spliced sequences may contribute to gene expression regulation as well as to increase the transcriptome and proteome diversity and genome extent (Blencowe 2017; Marasco and Kornblihtt 2022). AS can also be non-adaptive, as suggested by Xu and Zhang for alternative translation initiation (Xu and Zhang 2020).

The mechanisms involved in synthesizing different transcripts and isoforms vary among cell types and phases of development (Zeng, et al. 2006; Gutierrez-Arcelus, et al. 2015; Szafranski and Kramer 2015; Reber, et al. 2016) and have been associated with stress conditions, including temperature (Farashahi Yazd, et al. 2011; Shiina and Shimizu 2020; Dominguez, et al. 2022) and osmotic stresses (Natua, et al. 2022), reactive oxygen species overload (Cote, et al. 2012; Kumar, et al. 2019), hypoxia (Natua, et al. 2022) and acidosis (Mauduit, et al. 1999; Elias and Dias 2008; Rohani, et al. 2019; Natua, et al. 2022).

Literature has presented many data on the involvement of abnormal AS in the occurrence of several biological processes, such as normal ageing (Baralle and Romano 2023), premature ageing (Lopez-Mejia, et al. 2011) and age-related disorders, which range from hypertension to cardiovascular (Hu, et al. 2017; Gotthardt, et al. 2023) and liver diseases (Jobbins, et al. 2023), neurodegeneration (Nikom and Zheng 2023), and cancer (Song, et al. 2023; Temaj, et al. 2023). Aberrant splicing is also implicated in processes that affect people of all ages, such as inflammatory bowel disease (Zhou, et al. 2023; Zou, et al. 2023) and viral infection (Mann, et al. 2023). The mechanisms underlying the association of AS and diseases include alteration in splice site sequences and in cis- and trans-splicing regulatory elements (Tang, et al. 2020), chromatin modifications

(Gomez Acuna, et al. 2013) and mutations that disrupt RNA secondary structure (Warf and Berglund 2010), which can mediate mRNA decay or cause deletion of domains that are important for protein function. When compared to the consensus protein, alternative spliced isoforms may exhibit different subcellular or tissue localizations and divergent enzymatic activities, or interact with unusual ligands (Kjer-Hansen and Weatheritt 2023). Aberrant activity of splicing factors with multiple substrates may result in more broad and severe effects (Gotthardt, et al. 2023).

Specifically in cancer, AS can contribute to the transformation and progression processes, and to the response and resistance to therapy (Sciarrillo, et al. 2020). Upon analyzing data on 31 cancers, Zhang et al. (Zhang, et al. 2019) observed a number of splicing events associated with advanced-stage disease, survival and pathologic characteristics, which are potentially relevant as targets for diagnosis and therapies. The authors drew attention to the fact that, despite the huge number of splicing events in cancer, only few RNA variants and isoforms have been validated as directly involved in tumorigenesis.

In a previous study that assessed expressed sequences derived from head and neck cancer, we observed 788 potential new splicing variants in 748 different transcripts (Reis, et al. 2005). Analyzing these variants and members of their gene family, we found other 12 new splicing events, including a potential exon 2 skipping (AY562996.1 sequence, partial transcript, NCBI) of the *RIPK2* (receptor interacting serine/threonine kinase 2) gene. The human *RIPK2* gene has 11 exons spanning 33 kb of genomic sequence on chromosome 8q21.3. The full-length transcript (variant 1) encodes the RIP-2 isoform 1, whereas the variant 2 results in a potential truncated product with a partially deleted N-terminal and an intact C-terminal. It is generated by a splicing event that shifts the reading frame and results in several termination codons in downstream exons, while allowing translation from an alternative AUG in exon 3. Recent computational analysis supported by EST evidence predicted another *RIPK2* transcript variant, named X1, potentially generated by the skipping of exons 1 to 3 and partial inclusion of intron 3.

Receptor-interacting proteins (RIPs) are a family of serine/threonine kinases that integrate extra- and intracellular stress signals and share a homologous kinase domain at the N-terminus but have different C-terminal functional domains (He and Wang 2018; Cuny and Degterev 2021). RIP-2 (receptor-interacting serine/threonine-protein kinase 2) is a member of the RIP family and has received attention in recent years for its role in modulating immune responses to pathogens (Cuny and Degterev 2021; Eng, et al. 2021).

RIP-2 is expressed at high levels in several normal human tissues, such as skeletal muscle, but it is weakly expressed or absent in other tissues, including squamous epithelia (The Protein Atlas, version 23.0; Uhlen, et al. 2005). In most cancer types, *RIPK2* transcript and RIP-2 protein show differential activity in tumors compared to normal tissues, particularly in those that usually evolve in an inflammatory context, such as inflammatory breast (Zare, et al. 2018) and hepatocellular (Lu, et al. 2022) carcinomas. Amplification, missense or frameshift mutations and altered splicing of the *RIPK2* gene are more frequent in tumors, which suggests that RIP-2 has an oncogenic role in cancer (Zhang, et al. 2022). It has also been reported to promote dysfunction and remodeling of lymphatic vessels (Gambino, et al. 2017), processes that facilitate metastasis (Stacker, et al. 2014). Other recent data support its involvement in antitumor immune responses and immunotherapy resistance (Song, et al. 2022). Besides cancer, RIP-2 has also been associated with immune, inflammatory and nervous system diseases, such as systemic lupus erythematosus, allergic asthma, and amyotrophic lateral sclerosis (Tian, et al. 2023). These data evidence the role of *RIPK2* in processes active in several *pathological conditions, including cancer, and its potential as a therapeutic target*.

RIP-2 is the only member of the RIP family that, in addition to phosphorylating serine and threonine, is able to autophosphorylate tyrosine residues (Tigno-Aranjuez, et al. 2010; Chirieleison, et al. 2016). Its ATP- and substrate-binding sites are spread over much of the N-terminal, which contains a protein kinase-like domain (PKc\_like). At the C-terminal region is a caspase recruitment domain (CARD) (Inohara, et al. 1998), a binding module that interacts with NOD1 and NOD2 (nucleotide-binding oligomerization domain-containing protein 1 and 2, also called CARD-4 and CARD-5, respectively), which are intracellular receptors for innate immunity and are involved in sensing the presence of pathogens. After activation by bacterial peptidoglycans, NOD1 and NOD2 associate with RIP-2 via the CARD–CARD interaction and promote the expression of immune response and inflammatory genes through the nuclear factor kappa B (NF- $\kappa$ B) signaling (Inohara and Nunez 2003; Topal and Gyrd-Hansen 2021). NOD signaling may also cooperate with Toll-like receptors (TLRs) in

detecting bacteria (Kobayashi, et al. 2002), but there is no consensus on the mechanisms involved in the activation of RIP-2 by TLRs (reviewed by (Kurabi, et al. 2022)).

NOD pathway activation and cytokine production depend on RIP-2 polyubiquitination at several lysine residues, a process that requires XIAP (X-chromosome-linked inhibitor of apoptosis), a pivotal ubiquitin ligase in the NOD-RIP-2 inflammatory response. Although the kinase domain of RIP-2 is not functionally important for NOD signaling, it is correlated with NOD activation since RIP-2 autophosphorylation creates a substrate for the ubiquitin ligase binding process (Krieg, et al. 2009; Goncharov, et al. 2018; Topal and Gyrd-Hansen 2021).

Given that mutations and abnormal levels of the *RIPK2* transcript and RIP-2 protein are frequent in tumors and support their potential as molecular markers for cancer, and that RIP-2 kinase integrates extra- and intracellular stress signals and modulates immune and inflammatory responses, we investigated AS events that result in the deletion of the kinase domain. We also investigated the structure and expression of the *RIPK2* truncated variants and isoforms in different environments and in head and neck carcinoma, a type of tumor that evolves in an inflammatory context. In addition, we searched data throughout Supraprimates evolution that could support the biological importance of *RIPK2* alternatively spliced products. To the best of our knowledge, this is the first study on evolutive aspects and expression of *RIPK2* sequences arising through skipping of exon 2. Our results may stimulate other studies on these transcripts and isoforms and their associated interactions, involvement in biological processes and functional significance.

## Results

### In-silico Splicing Analysis

**Table 1** reports the human transcripts and proteins of *RIPK2*, Gene (NCBI) and UniProt accession numbers, lengths in base pairs (bp) or amino acids (aa), masses (Da), AS types that result in the deletion of the kinase domain, as well as exons and introns *involved* in the AS. Transcript alignments (variants 1 and 2, predicted variant X1 and AY sequence) performed by BLAT are shown in **supplementary fig. S1A, Supplementary Material** online.

The human full-length variant 1 (NM\_003821.6) encodes a 61.2 kDa protein (RIP-2 isoform 1; NP\_003812.1) with two domains: a PKc\_like domain and a CARD domain located at amino acids 20 to 303 (exons 1 to 6) and 438–524 (exon 11), respectively. Human variant 2 (NM\_001375360.1) is derived from the skipping of exon 2, which alters the reading frame, producing several premature stop codons (**supplementary fig. S1B, Supplementary Material** online). A partial sequence

**Table 1**

Transcripts and correspondent protein products of human RIPK2. Accession numbers, gene length in nucleotides (bps), number of amino acids (aa), mass (Da), alternative splicing (AS) type, exons/introns involved in the AS, and kinase domain location of RIPK2 isoforms, according to Gene (NCBI) and Uniprot databases, and to Conserved Domains annotation resource from BLAST search tool

Transcript	Protein	Transcript—Gene (NCBI) accession number	Protein—UNIPROT/Gene (NCBI) accession number	Gene Length (bps)/number ofaa	Mass (Da)	AS type <sup>a</sup>	Exons/ Introns involved	Kinase domain (aa)
Variant 1	Isoform 1	NM_003821.6	O43353-1/NP_003812.1	2516/540	61,195	...	...	20-303
Variant 2	Isoform 2	NM_001375360.1	O43353-2/NP_001362289.1	2362/403	45,582#	ES	2/-	1-166
Variant X1 <sup>b</sup>	Isoform X1 <sup>b</sup>	XM_011517357.3 <sup>b</sup>	-/XP_011515659.1 <sup>b</sup>	1889/369 <sup>b</sup>	41,571 <sup>b</sup>	IR	1 to 3/3	1-132
AY sequence	Isoform b	AY562996.1	-/AAS75586.1	302/41	...	ES	2/-	...

<sup>a</sup>AS type: ES = exon skipping; pIS = partial intron retention.

<sup>b</sup>PREDICTED.

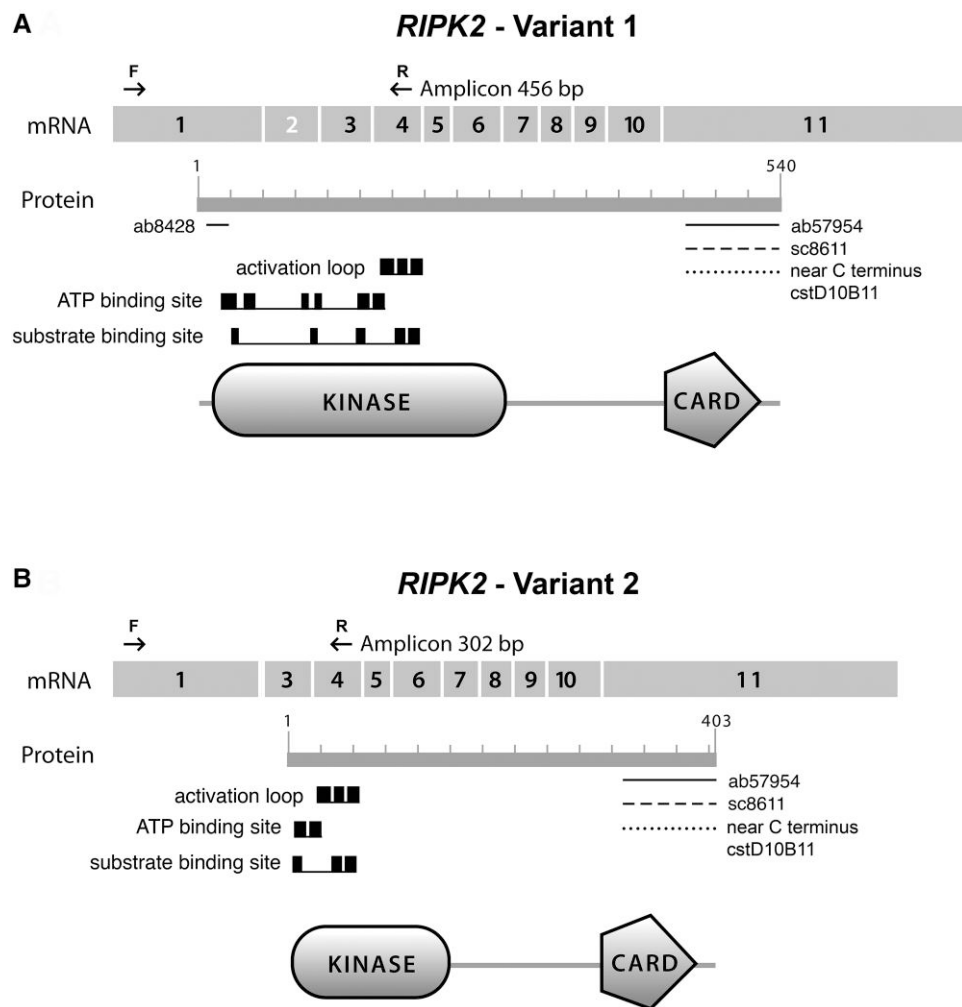


**Fig. 1.**—Diagram of splice variants and isoforms of human *RIPK2*. a) The variant/transcript 1 encodes the longer isoform 1 and b) the variant 2 presents skipping of exon 2 and encodes a truncated product (isoform 2) with a partially deleted kinase domain and an intact caspase recruitment (CARD) domain. Arrows indicate the positions of the forward primer A and reverse primer B for conventional PCR expression analysis, and horizontal bars below the isoform 1 and 2 indicate the epitope region for anti-RIP-2 ab8428, ab57954, sc8611 and cstD10B11 used in the present study.

of this variant was previously submitted by us to NCBI (GenBank accession number AY562996.1). Translation of variant 2 starts in an in-frame alternative AUG (nucleotides

85 to 87 of exon 3) and gives rise to the 45.6 kDa RIP-2 isoform 2 (NP\_001362289.1; 403 aa) with a short PKC<sub>like</sub> domain of 166 aa (Fig. 1). Another N-truncated variant

has been predicted by automated computational analysis (variant X1; XM\_011517357.3) using the gene prediction Gnomon method, and it is supported by EST evidence (according to NCBI, GenBank; [www.ncbi.nlm.nih.gov/nuccore/XM\\_011517357.3/](http://www.ncbi.nlm.nih.gov/nuccore/XM_011517357.3/)). The variant X1 shows loss of exons 1 to 3, partial retention of intron 3 and a downstream in-frame AUG codon (nucleotides 31 to 33 of exon 4; [supplementary fig. S1B, Supplementary Material](#) online), potentially generating a protein with a smaller PKC<sub>like</sub> domain of 132 aa (XP\_011515659.1).

The TCGA SpliceSeq tool confirms the skipping of exon 3 (corresponding to exon 2 of the NCBI NM\_003821.6 sequence) in head and neck squamous carcinoma ([supplementary fig. S2, Supplementary Material](#) online). SpliceSeq also proposes the skipping of a new exon, exon 2 (derived from intron 1 of NCBI sequence), but with a low PSI (Percent Spliced-In or percent of exon inclusion) value. Differences in exon numbering between SpliceSeq and NCBI data occur because SpliceSeq merges the known transcripts into a unified transcript splice graph, which may result in a numbering different than those used by other databases, including NCBI.

A multi-sequence alignment analysis using the UCSC browser showed that *RIPK2* gene is well conserved across vertebrates ([supplementary fig. S3, Supplementary Material](#) online). To gain insight into mammalian spliced transcripts, we analyzed in detail exons 1 to 3 and introns 1 and 2, and the corresponding isoform sequences in 12 mammals of superorder Euarchontoglires, also called Supraprimates (human, chimpanzee, gorilla, orangutan, gibbon, Rhesus, flying lemur, hare, pika, mouse, rat, tree shrew), and in *Canis lupus familiaris* of superorder Laurasiatheria (as an outgroup) ([supplementary File S1, Supplementary Material](#) online, pages 3 to 85; [supplementary fig. S4, Supplementary Material](#) online). Despite millions of years of divergence between these species, the sequence alignments of exons 2 and 3 showed high identity (an average of ~95%) comparing 29 transcripts with the consensus NM\_003821.6 transcript (*Homo sapiens*). Otherwise, the exon 1 sequence evolved toward different base compositions ([supplementary table S1, Supplementary Material](#) online).

Alignment by BLAT Genome Browser and BLAST Global Alignment Tool revealed that human, chimpanzee, gorilla and tree shrew have a similar reviewed or predicted variant derived from the exon 2 skipping, which alters the reading frame and allows protein translation to initiate from an AUG in exon 3. These truncated transcripts, except the human variant 2, also showed a partial skipping of exon 1. Variants of other Supraprimates (X3 in hare, X2 in pika and rat) exhibited partial exon 2 skipping accompanied by exonization of the next intron and exon 1 deletion, resulting in an in-frame TIS in exon 3 and in a similar truncated protein at the N-terminus. An only event, intron 2 exonization in the mouse variant 2, showed the same result. A TIS

in exon 2 associated with intron 1 exonization and partial skipping of exon 1 was observed in variants X3 and X1 of Rhesus and rat, respectively, which resulted in a truncated but longer putative N-terminus compared to that in the human variant 2. Inversely, the human transcript X1 showed a drastic deletion in the N-terminus involving exons 1 to 3 ([supplementary table S1, Supplementary Material](#) online). Similarities between truncated variants found in ten mammals and the human consensus sequence (variant 1) are shown in [Fig. 2](#). Besides of the ten mammals analyzed in details, other Supraprimates may exhibit similar truncated variants and isoforms, such as rabbit (*Oryctolagus cuniculus*, XM\_051844621.1 and XP\_051700581.1) and tarsier (*Carlito syrichta*, XM\_021713646.1 and XP\_021569321.1). Differently, *Canis lupus familiaris* shows a dissimilar structure at the 5'-terminal region of *RIPK2*, with a new exon and a more upstream TIS position.

At the amino acid level, the truncated isoforms that exhibit the TIS in exon 3 shared ~75% sequence percentage identity with the consensus isoforms (from the same mammal) ([supplementary table S1, Supplementary Material](#) online), a result that is mostly due to the loss of spliced or deleted N-terminal regions. Considering independently each specie, exon 11 was not involved in deletion or skipping events that could result in changes of the CARD size ([supplementary fig. S4, Supplementary Material](#) online; [supplementary File S1, Supplementary Material](#) online, [pages 81 to 85](#)).

To evaluate the efficiency (E) of TISs of mammalian *RIPK2* transcripts, we compared the Kozak sequences flanking AUG codons (Kozak 1986) with the sequences described by Noderer et al. (Noderer, et al. 2014). According to the data generated by these authors, the Kozak sequence in exon 3 has E values of 91 to 107, and the one in exon 1 has E values of 90 to 106 ([supplementary table S1, Supplementary Material](#) online). The potential Kozak sequence with an AUG (in frame) in exon 2 ([supplementary fig. S1B, Supplementary Material](#) online) has E values of 53 to 60.

In brief, different events associated with a reduction of the RIP-2 kinase domain were observed, including partial or total exon skipping, exon deletion, and exonization of intron segments. No associations were found between alternative spliced exon 2 and exon/intron size, Kozak sequence or splice site motifs.

### Expression Patterns of the Human *RIPK2* Transcripts and Isoforms

*Expression of human RIPK2 transcripts in normal and tumor samples.* *RIPK2* transcripts 1 and 2 were co-expressed in normal brain, testis, heart, lung, stomach, kidney, larynx, liver and tongue tissues ([Fig. 3A](#)). Both transcripts were also detected in tumor and tumor-free surgical resection



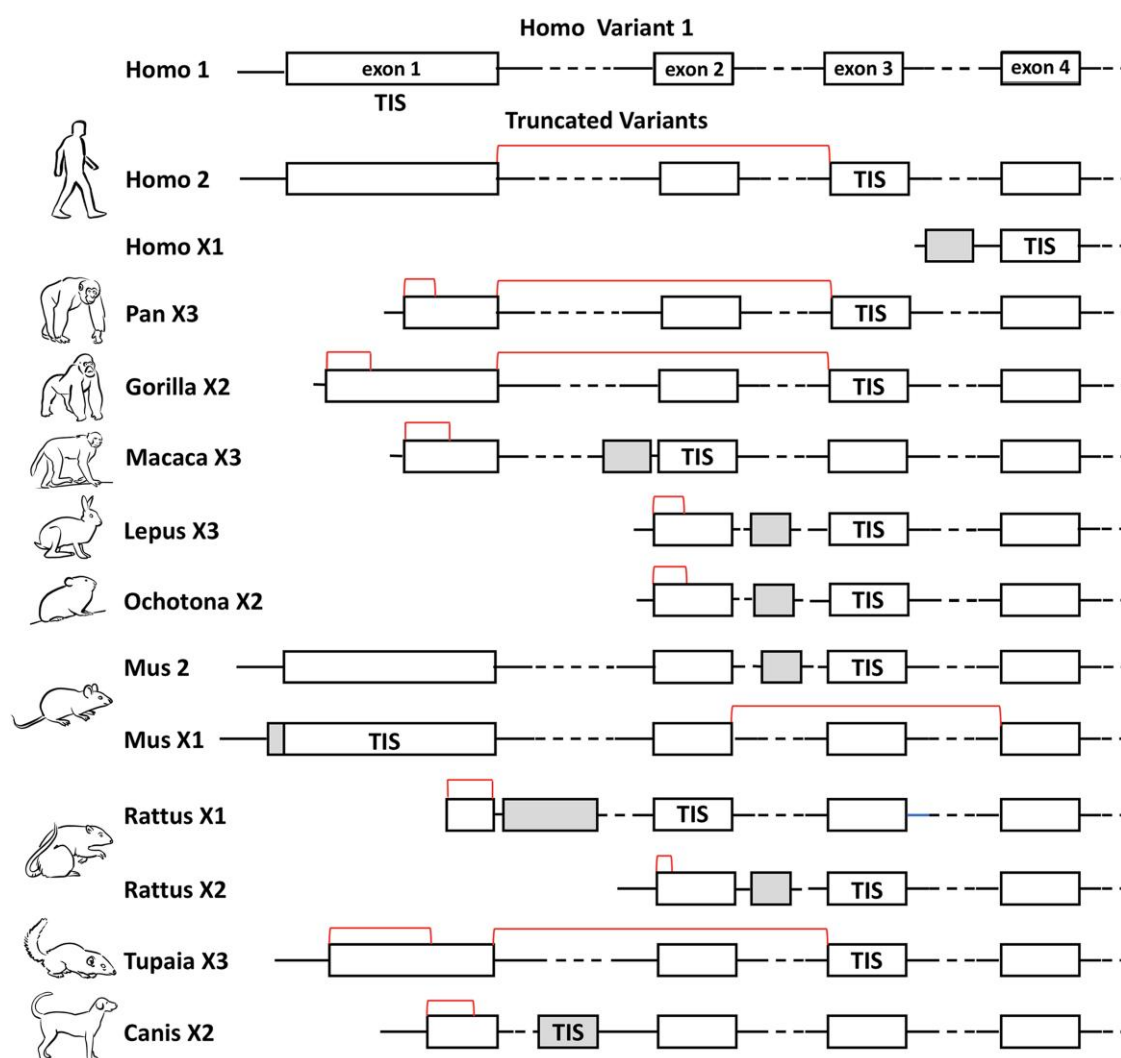


**FIG. 2.**—Schematic representation of the 5'-terminal region of *RIPK2* truncated transcripts observed in 10 mammals compared to the human consensus sequence (variant 1). Truncated variants from *Homo sapiens* (2 and X1), *Pan troglodytes* (X3); *Gorilla gorilla gorilla* (X2); *Macaca mulatta* (X3); *Lepus europaeus* (X3); *Ochotona curzoniae* (X2); *Mus musculus* (2 and X1); *Rattus norvegicus* (X1 and X2); *Tupaia chinensis* (X3); and *Canis lupus familiaris* (X2). Boxes represent exons, lines represent introns, potential exonization of introns or 5'UTR sequences are illustrated as gray boxes; potential intronization of sequences (total or partial exon skipping) are indicated by red brackets. TIS = translation initiation site.

samples from patients with oral SCC, as illustrated by five matched samples in Fig. 3B.

The in-silico analysis using gnomAD dataset, which aggregates human exome and genome sequencing data from several large-scale sequencing projects, found very low allele frequencies in splice regions of introns 1 and 2. The data of the GTEx project also showed that *RIPK2* is expressed across many human tissues and exon 3 (that corresponds to exon 2 of the NCBI sequences) is less expressed than the other exons, which may be explained by two variants with different expression profiles.

Quantitative real-time PCR detected no difference in the expression of full-length transcript 1 between 16 tumors and their respective surgical margins, whereas significantly

increased levels of transcript 2 were observed in tumor versus margin samples (Fig. 3C). Supporting these results, the SpliceSeq analysis showed that exon 3 (corresponding to exon 2 of the NM\_003821.6 sequence) has higher PSI (percent of exon inclusion) values in normal samples than in tumor samples from the TCGA head and neck neoplasm cohort (supplementary fig. S2C, Supplementary Material online).

**Expression of human RIP-2 isoforms in normal and tumor samples.** In tissue samples from tongue, mouth floor and larynx carcinomas, Western blots with antibodies sc8611 and ab57954 directed against the C-terminal region of RIP-2 showed a band at ~55 kDa that corresponds to isoform 1, but no band at ~41 to 45 kDa was observed (Fig. 3D-G). Unlike transcript 1 that showed no difference

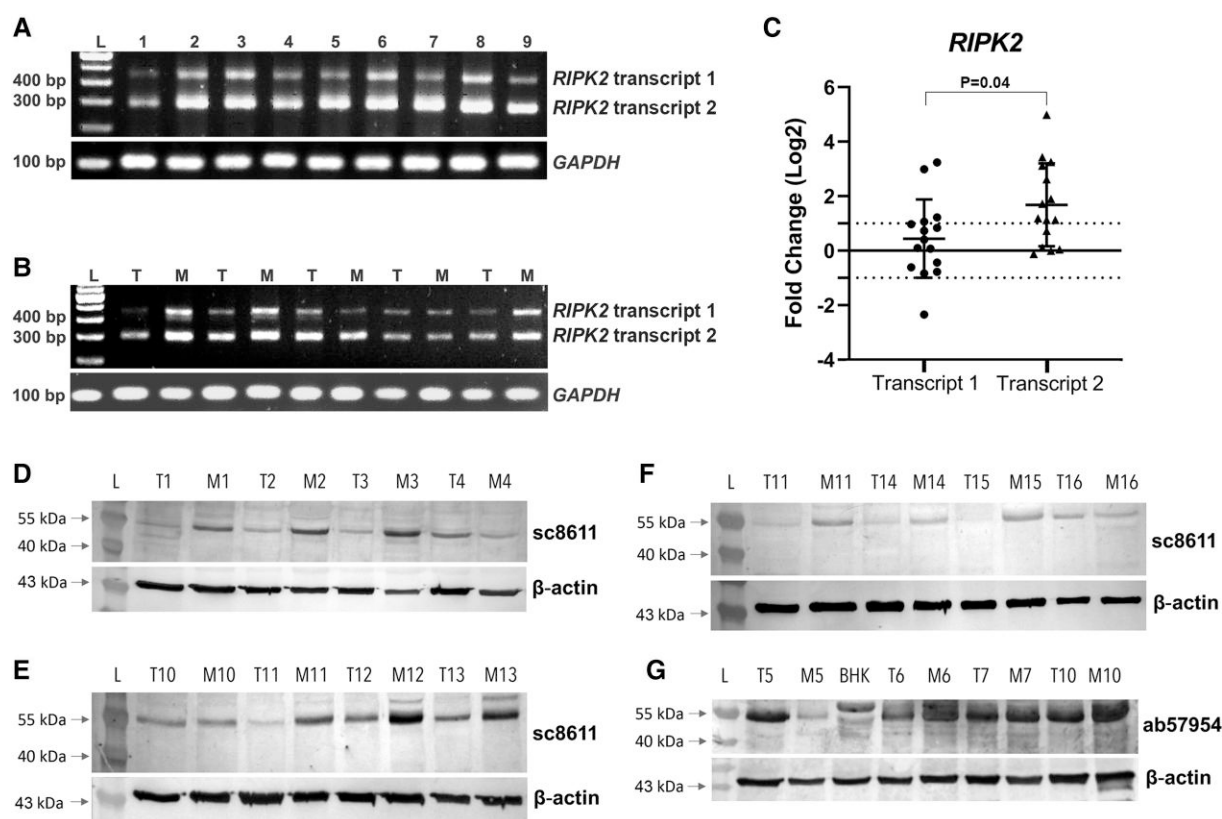


**Fig. 3.**—Human *RIPK2* variant and RIP-2 isoform expression in normal tissues, and in oral and laryngeal SCC samples. a-b) Conventional PCR products from *RIPK2* transcript 1 (456 bps), transcript 2 (302 bps), and GAPDH (101 bps) in: a) normal human tissues: 1 = brain, 2 = testis, 3 = heart, 4 = lung, 5 = stomach, 6 = kidney, 7 = larynx, 8 = liver, 9 = tongue; b) samples from patients with oral cancer: T = tumor; M = resection margin; L = 100-bp fragment size marker. c) RT-PCR performed in triplicates to evaluate the expression of *RIPK2* transcripts 1 and 2 in 16 oral cancer samples (T) and resection margins (M). Transcript 2 showed a higher expression than transcript 1 in tumors normalized with matched resection margins ( $P=0.04$ , unpaired t test); ACTB as the expression reference. d-g) Western blot analysis of RIP-2 expression in oral and laryngeal SCC samples using anti-RICK sc8611 (N-terminus) and ab57954 (C-terminus) antibodies. Increased expression of the isoform 1 (~55 kDa) in several margin (M) compared to tumor (T) samples. g) A sharp ~61 kDa band corresponding to isoform 1 in BHK-21 cells and a ~55 kDa band in margin and tumor samples. Normalization controls:  $\beta$ -actin. L = Protein Ladder; T1/M1—T9/M9 = oral SCC samples; T10/M10—T17/M17 = laryngeal SCC samples.

in the expression level between tumors and their respective surgical margins, isoform 1 was apparently more expressed in margins than in tumors, an inverse profile compared to transcript 2.

It must be emphasized that Western blot analysis using different antibodies, concentrations of antibody, samples and exposure times generally showed weak signals for RIP-2, unlike for the housekeeping proteins. To address this point, we also evaluated a mammalian cell line of a different lineage (BHK-21/CCL-10, hamster fibroblasts, ATCC), which exhibited a sharp ~61 kDa band, but also no well-defined signal for isoform 2 (Fig. 3G).

Despite the detection of transcripts 1 and 2 and the in-silico prediction of RIP-2 isoforms, spliced transcript 2 was not (or was only minimally) translated into protein in the normal human tissues and cancer samples. No isoform was identified by mass spectrometry (MS) analysis of the gel slice containing the 41 to 45 kDa bands, a

result that may be related to a low limit of detection (Gross 2017).

The band at ~8 kDa, previously observed by Krieg and collaborators (Krieg, et al. 2009) in the human embryonic kidney cell line HEK 293T, was not observed in our blots. To date, this small isoform has not been referred to by other investigators or predicted by the Gene (NCBI) or UniProt databases.

*Expression of human RIPK2 transcripts and isoforms under temperature stress conditions.* A previous pilot study was conducted on three cell lines (FaDu, SiHa and Hep-2) to investigate whether AS of *RIPK2* is induced or inhibited by temperature (40 °C, 17 °C and 5 °C) and acid (atmosphere of 10% CO<sub>2</sub>) stresses. In conventional PCR, no effect of pH on the expression of either transcript was observed in the three cell lines. In contrast, heat/cold stress apparently affected *RIPK2* transcript expression only in FaDu cells (supplementary fig. S5, Supplementary Material online), a

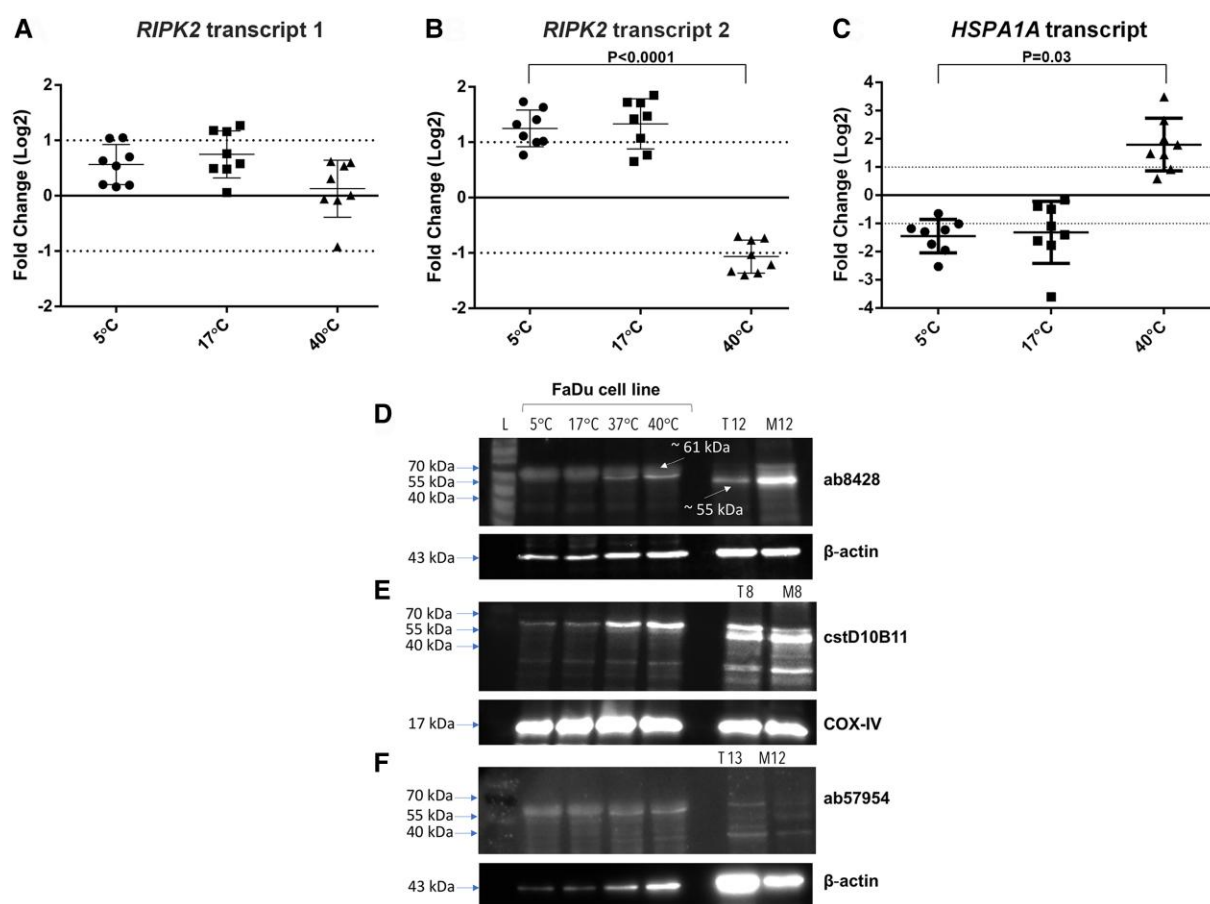


**Fig. 4.**—Human *RIPK2* mRNA expression in cells under temperature stress conditions. a-b) RT-PCR assays were performed in triplicates to evaluate the level of human *RIPK2* transcripts 1 and 2 in cells under heat/cold conditions. Temperature stress induced a significant increase in transcript 2 expression level at lower temperatures and a decrease at a higher temperature ( $P < 0.0001$ , unpaired t test), but no effect on transcript 1 expression was observed (control cells at 37 °C as the calibrator sample; *TUBA1C* as the expression reference). c) *HSPA1A* showed elevated levels at 40 °C ( $P = 0.03$ , unpaired t test) (*TUBA1C* as the expression reference). Values were log2 transformed (y-axis) so that all values below  $-1$  indicate downregulation in gene expression while values above 1 represent upregulation. The error bar represents the mean  $\pm$  S.E.M (standard error of the mean). d-f) Western blot analysis of human RIP-2 expression in cells under stress conditions by anti-RIP-2 ab8428 (N-terminus), cstD10B11 and ab57954 (C-terminus) antibodies. In FaDu cell line under temperature stress, a reduced isoform 1 expression was observed at 5 °C or 17 °C compared to control cells. Normalization controls:  $\beta$ -tubulin and COX IV. L = Protein Ladder.

result that can be cell line dependent. RT-PCR confirmed an increase in the transcript 2 expression level at lower temperatures and a decrease at a higher temperature, but no changes were observed for transcript 1 in FaDu cells (Fig. 4A and B). The findings for transcript 2 could be justified by the occurrence of cell death under heat stress conditions. However, the control for the heat/cold experiment, *HSPA1A*, showed elevated levels at 40 °C (Fig. 4C), indicating that the degree of cell death was not significantly increased at temperature extremes.

Western blot analysis using the N-terminal domain anti-RIP-2 ab8428 demonstrated an immunoreactive band at ~61 kDa, consistent with the molecular weight of isoform 1 (61,195 Da), but as expected for the N-terminus anti-RIP-2, no band at 41 to 45 kDa (isoform 2 and X1) was detected (Fig. 4D). A band at ~61 kDa was also observed using the

C-terminal domain anti-RIP-2 sctD10B11 and ab57954, and again no sharp band at ~41 to 45 kDa was visualized (Fig. 4E and F).

In heat/cold stress experiments, lower expression of isoform 1 was observed in cells maintained at low temperatures than in control cells at 37 °C, and relatively higher expression was observed at 40 °C. However, a similar expression profile was visualized for  $\beta$ -actin (Fig. 4D and F), indicating that this protein is also sensitive to temperature changes and cannot be used as a housekeeping gene in the heat stress assay. Thus, four other normalization controls were evaluated:  $\beta$ -tubulin, COX IV, GAPDH and histone H3 (supplementary fig. S6, Supplementary Material online). COX IV and histone H3 showed low variation after heat/cold stress, and COX IV was chosen as the most reliable control. Using COX IV as a housekeeping, a very small



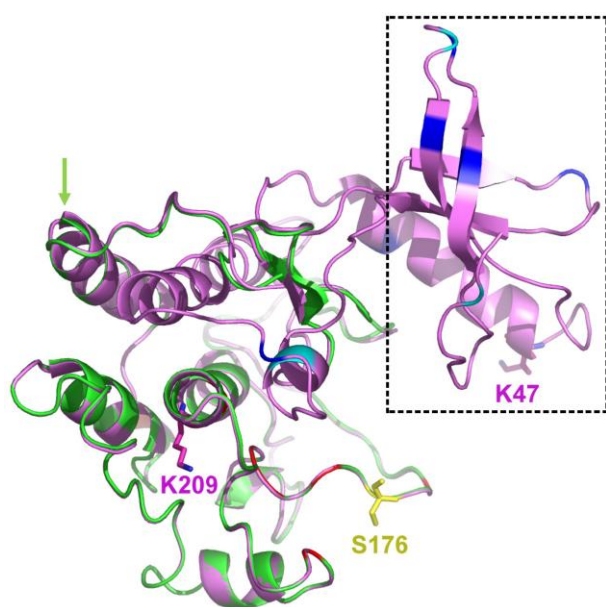


**Fig. 5.**—Homology modeling of the catalytic domain of human RIP-2 isoforms. Superposition of the models built for the RIP-2 isoforms 1 and 2 (ribbon diagram colored in magenta and green, respectively), with part of the kinase domain highlighted by the dashed box (present only in isoform 1), and the superposition of the isoform 1 and 2 models outside the box. Isoform 2 lacks the first 137 amino acids of RIP-2 and, consequently, the residue critical for kinase activity of RIP-2 (lysine K47). The isoform 2 start is indicated by a green arrow. Ten phosphorylation sites (serine and threonine residues, respectively) predicted for isoform 1 and absent in isoform 2 sequence are indicated in blue and cyan inside the dashed box. Serine S176 is shown in yellow stick, and is indicated to be conveniently accessible to the solvent and to phosphorylation. Lysines K47 and K209 are also shown in colored sticks.

or no effect of hyperthermia was observed for the ~61 kDa band corresponding to isoform 1, but a reduced expression was observed at 5 °C or 17 °C (Fig. 4E).

### Protein Sequence Alignment and Homology Modeling Procedures

The model built for the catalytic domain of human isoforms 1 and 2 showed good stereochemical quality (Fig. 5—part of the kinase domain present only in isoform 1 inside the *dashed box*; superposition of the isoform 1 and 2 models outside the box). Despite overall low sequence identity among the complex structures of the homolog RIP-2 proteins, the active sites were structurally similar and reasonably well conserved. The model built for isoform 1 was 128 residues larger than the one obtained for isoform 2 and included L10 to T296 of the overall sequence. On the other hand, isoform 2 included methionine M129 to threonine T296 of the overall sequence. Regarding the phosphorylation sites predicted for isoform 1, the NetPhosK 1.0 server identified 10 sites that are absent in the isoform

2 sequence: serines at positions 8, 25, 29, 33, 58, 76, and 102 and threonines at positions 12, 31, and 95. The study of Dorsch's group (Dorsch, et al. 2006) suggested that S176 is an important autophosphorylation site for RIP-2 and that this phosphorylation can be used to monitor the activation state of RIP-2. Figure 5 shows the superposition of the two models as well as the localization of S176, which seems to be conveniently accessible to the solvent and to phosphorylation. K47 in the conserved ATP-binding site and the critical polyubiquitination site K209 are also shown in Fig. 5. The rationale for this analysis was to identify potential changes in protein features. Although isoform 2 was not detected in our samples, it may be expressed in another cell type or condition.

## Discussion

### Conservation of the Alternatively Spliced N-terminal Region of *RIPK2*

It is well known that AS is an important mechanism for functional and protein expression and diversity. The present study aimed to shed light on the conservation of the alternatively spliced exon 2 of *RIPK2* in mammals belonged to the five orders of Supraprimates (Primates, Dermoptera, Lagomorpha, Rodentia, Scandentia) and to the Carnivora order (dog), analyzing the information about AS-derived variants and isoforms that have been reviewed or predicted by NCBI. The tree shrew (Scandentia order) was especially important for our proposal because it is a potential animal model for several human diseases and because its genomic data show that the nervous, immune and metabolic systems are similar to those of humans (Fan, et al. 2013; Sanada, et al. 2019). In fact, tree shrew is more similar to primates than to rodents in terms of immunity. Upon infection by microorganisms, tree shrew receptors, including NOD and TLRs, induce the production of cytokines and inflammatory factors. Many of these receptors and their effectors have high homology with those in primates (Lu, et al. 2021) and, therefore, can interact with RIP-2 to promote immune responses.

Alignment of *RIPK2* transcripts by BLAT and BLAST tools showed that members of the families Hominidae and Tupaiidae, two groups with divergence time of 70 to 80 million years (Shao, et al. 2023), have the same exon 2 skipping that leads to a frameshift and changes the translation initiation resulting in a shorter putative protein. At first glance, the presence of the same AS in Hominidae and Tupaiidae suggests the hypothesis that it was present in a common ancestor (Gelfman, et al. 2012). However, a similar truncated sequence was detected in other mammals, but associated with different events: partial or total exon deletion, exonization, and partial exon skipping. The long intron 1, which is present in all mammals analyzed, may explain

the results. In fact, large distances between contiguous exons can influence the splice site recognition and the spliceosomal assembly, increasing the probability of AS (Fox-Walsh, et al. 2005). In brief, different mechanisms related to or associated with AS events promote partial deletions of the putative RIP-2 N-terminal in Supraprimates, leading to a shorter kinase domain size and loss of ATP and substrate binding sites. Interestingly, similar events were not found in exon 11 that encodes the CARD domain.

These findings raise challenging questions: Why the truncated *RIPK2* variants have been selected? Are the truncated variants non-coding RNAs with high decay rates or regulatory activities? Do the truncated variants encode functional proteins that are expressed in specific tissues or developmental stages? What the adaptive advantage for a truncated kinase domain?

The predominance of the kinase domain deletion of potential RIP-2 isoforms fits with the hypothesis of AS “hot-spots” that are selected during mammalian evolution (Xing and Lee 2005). Our suggestion is that, in Supraprimates, different mechanisms acting on a specific transcript region led to the same effect, i.e. the usage of a downstream TIS. The advantageous effects were selected and converged toward the partial deletion of the RIP-2 N-terminal.

### Expression of Human *RIPK2* Transcripts and Isoforms in Normal and Tumor Samples

*RIPK2* transcripts 1 and 2 were co-expressed in normal tissue samples. In tumor samples, our results showed discordant expression patterns of *RIPK2* transcripts 1 and 2. The ratio of transcript 1 to transcript 2 was lower in tumor than in margin samples, with transcript 2 (but not transcript 1) exhibiting higher expression in tumors than in their respective surgical margins.

At the protein level, isoform 2 was not detected in any of our samples, and most tumors showed reduced expression of isoform 1, a result concordant with the report by Wang and collaborators (Wang, et al. 2014). These authors analyzed oral SCCs by immunohistochemical techniques to reveal the presence of RIP-2 protein using a mouse monoclonal anti-RIP-2 antibody from Abcam, one of the antibodies used in the present study. Although the authors clearly showed that the expression of RIP-2 decreases with the progression of OSCC, their results did not elucidate the contribution of each RIP-2 isoforms since the antibody is unable to differentiate between them by immunohistochemical techniques with only an antibody against an immunogenic peptide. In contrast to Wang et al., the present study focused on detecting *RIPK2* protein products using Western blotting with several antibodies and included oral and laryngeal subsites.

Zhang and collaborators (Zhang, et al. 2022) observed that the levels of RIP-2 protein were significantly higher in

several tumors than in the corresponding normal tissues. The protein expression presented by Zhang et al. was determined using the immunohistochemical data from the Human Protein Atlas (HPA) database. However, the HPA (version 23.0; Uhlen, et al. 2005)) results show moderate, weak or negative intensity of RIP-2 in HNSCC, an heterogeneous group of more than ten anatomical subsites.

The different expression profiles observed for transcript 1 (similar expression in tumor and margin samples) and the corresponding protein isoform 1 (upregulation in margin samples) can be explained by the fact that protein abundance may differ from mRNA expression, mainly because of posttranscriptional control of gene expression or protein half-lives (Greenbaum, et al. 2003; Kuchta, et al. 2018). The high levels of transcript 2 and low levels of protein isoform 1 in tumors compared to normal tissues may also represent a random finding or a regulatory relationship.

Differences in AS between tumor and normal samples have been widely described in the literature. For example, Gracio et al. (Gracio, et al. 2017), using ExonArray analysis of breast cancer and normal breast tissue samples, identified more than 200 genes with splicing differences associated with clinical outcome. Other studies using the TCGA BRCA cohort have also provided significant results, such as the one described by Bjørklund et al. (Bjørklund, et al. 2017), who reported AS events specific for invasive breast ductal carcinoma in five genes after validation in patient samples. Pani et al. (Pani, et al. 2021) also detected AS events in the sphingolipid gene *CERS* and showed the potential of this gene as a marker for diagnosis and survival in breast cancer subtypes. A large study by Kahles et al. analyzed 32 cancer types, including head and neck cancers, using RNA and whole-exome sequencing data and observed many differences in AS events in cancer compared to normal cells (Kahles, et al. 2018). Specifically, in regard to head and neck cancer, several groups have described genes with differential expression of spliced variants (Sam, et al. 2012; Liborio, et al. 2013; Palve, et al. 2014; Radhakrishnan, et al. 2016; Brady, et al. 2017), among others). However, to the best of our knowledge, this is the first report showing differential expression of *RIPK2* transcript 2 and isoform 1 between oral and larynx carcinomas and normal tissues.

### Regulatory Mechanisms Involved in AS and Translation Initiation

Dasgupta and collaborators (Dasgupta, et al. 2008) described a C-terminal fragment of a member of the RIP family, RIP-1, that can activate signaling events, including the NF- $\kappa$ B and TNF pathways. They concluded that the short RIP-1 with a deleted N-terminus affects long isoform levels and may represent a new regulatory mechanism. Although they exhibit some differences, RIP-1 and RIP-2 participate in the same regulatory metabolism; therefore, RIP-2 isoform 2, if

translated, might have a similar function and modulate full-length RIP-2 in other tissues and under different conditions.

Interestingly, Callow et al. (Callow, et al. 2018) observed that PTBP1, an RNA binding protein, controls RIPK1 protein abundance by determining alternative splice site selection and proposed that this type of regulation might be used by developmental processes, cell death modulation or stress-response pathways. To our knowledge, no similar *RIPK2* AS regulation is known.

It is tempting to speculate that the AUG codon of *RIPK2* transcript 1 may modulate translation of the downstream transcript 2, as cited for stress-response mRNAs in the literature (Spriggs, et al. 2010; Andreev, et al. 2018). The intercistronic region between both ORFs should be long enough to support ternary complex (eIF2-GTP-Met-tRNAi) reacquisition and downstream AUG recognition by the scanning ribosome subunit (Kozak 1987). Li et al. (Li, et al. 2022) evaluating more than 13,000 yeast variants also observed that out-of-frame downstream AUGs can inhibit translation at the annotated AUG depending on the distance between them.

The usage of noncanonical AUG initiation sites has been explored recently as a potential therapeutic approach. For example, Bowling et al. (Bowling, et al. 2022) investigated the cystic fibrosis transmembrane conductance regulator (*CFTR*) gene and observed that N-terminal variants undergo downstream translation initiation, resulting in escape from nonsense-mediated mRNA decay and in the generation of stable transcripts. The authors hypothesized that these variants may be used for recovery of *CFTR* gene function via combination of translation readthrough promotion at stop codons and protein modulator therapy.

Using numeric scores based on TIS efficiencies defined in mammalian cells by Noderer et al. (Noderer, et al. 2014), we determined that TISs in exon 1 and exon 3 have good E values (90 to 107), and therefore both have a high probability to initiate the translation of transcripts 1 and 2, respectively. However, a well-defined expression of the short protein isoform was not observed in the analyzed cells and tissues. Literature data have demonstrated that several factors may affect the translation reinitiation occurring at a downstream TIS. For example, the distance between the upstream and downstream sites, if short or long, may facilitate or inhibit reinitiation. A similar effect has been cited for the presence of a terminator codon that halt translation and allow restart. Competence of ribosomal subunits is also another factor since some subunits detach and others remain bound to the mRNA and may resume scanning (Kozak 1986; Hernandez, et al. 2019).

### Expression of Human *RIPK2* Transcripts and Isoforms Under Stress Conditions

In the present study, we observed different expression patterns of transcripts and isoforms in FaDu cells under

temperature stress conditions: variant 1 expression was insensitive to low or high temperatures. In contrast, variant 2 was upregulated at 5 °C or 17 °C and downregulated at 40 °C compared to control conditions. Isoform 2 was not detected in any of these conditions.

The band sizes and levels of isoform 1 in cell lines analyzed by Western blot assays were different than those observed in tissue samples, which may be explained by dissimilar posttranslational modifications or cleavages in distinct contexts. Concerning SiHa and HEp-2 cells, variant 1 and 2 expression levels were not clearly affected by heat/cold stress or by acid stress.

It is well known that all organisms from prokaryotes to higher eukaryotes, including bacteria, yeast, plants and animals, respond to heat and cold stress by changing transcription, translation, signaling and other metabolic processes (Al-Fageeh and Smales 2006). The hyperthermia response involves molecular chaperones called heat-shock proteins (HSPs) that repair conformational changes or trigger degradation of damaged proteins and represent a defense response to adverse conditions (Paszek, et al. 2020; Ruta, et al. 2021). HSPs are classified into families based on their molecular weight, with HSP70 being the best characterized. HSPA1A is a stress-inducible member of the HSP70 family that is constitutively expressed at low levels but upregulated when cells are subjected to adverse conditions, such as heat shock (Vostakolaei, et al. 2021).

Hyperthermic stress effects have been studied in many organisms, and cell line models. The examples include clinical responses in humans (Wetsel 2011; Cui and Sinoway 2014), transcriptome alterations in *Caenorhabditis elegans* (Xu, et al. 2023), *Drosophila*, yeast, mouse, human (reviewed by (Pessa, et al. 2024)), and in cancer cells (Scutigliani, et al. 2022). In contrast, cold-shock stress has been less well investigated, and little is known about the underlying mechanisms involved in responses to hypothermia, which can occur as a response to a drug, disease or exposure to the cold. The literature suggests that mild hypothermic conditions induce or inhibit the synthesis of specific proteins, an effect that is cell line/tissue dependent (Tait, et al. 2013; Adjirackor, et al. 2020; Baudier and Gentil 2020). In microorganisms, mistranslated proteins synthesized at low temperatures are apparently well tolerated and even beneficial to cells (Han, et al. 2020). Focusing on stem cells, the literature survey by Farashi and Sharifi (Farashi and Sharifi 2021) proposed potential mechanisms involved in the response to temperature changes. The survey conclusions suggested that hypothermia enhances cell adhesion, proliferation and survival, reducing oxidative stress and preventing apoptosis.

### Regulation of AS by Stress Conditions

Regarding AS regulation by temperature and other stressors, a significant amount of data has already been published.

For example, Gemignani and collaborators (Gemignani, et al. 2002) observed a shift in splicing of a mutated human  $\beta$ -globin gene affected by temperature in vitro, which led the authors to propose temperature changes as a treatment for  $\beta$ -thalassemia. Farashahi Yazd's group (Farashahi Yazd, et al. 2011) also described a novel spliced variant of the *OCT4* gene (or *POU5F1*) whose expression was significantly elevated under heat stress conditions and suggested a potential role of the transcript (*OCT4B1*) and its product in mediating temperature responses and apoptosis. In the same line of investigation, Horii et al. (Horii, et al. 2019) observed that hypothermia modulates AS of the *Cirbp* (inducible RNA binding protein) gene in mice and suggested that the long isoform may function as a dominant-negative isoform. In *Drosophila*, Telonis-Scott et al. (Telonis-Scott, et al. 2014) showed that products of *starvin*, a thermally responsive gene with seven transcripts and five proteins derived from alternative transcription and AS, present distinct phenotypes: the largest and least heat-responsive isoforms have geographic and temporal profiles, while the highly heat-inducible isoforms are mostly conserved across populations. These data demonstrate how complex and broad thermal stress responses are, a subject that, according to Telonis-Scott and collaborators, deserves an approach that goes beyond the gene level.

Under stress, *RIPK2* transcripts generated by AS could disturb RIP-2 isoform 1 expression. It is known that abnormal RIP-2 levels affect immune responses (Kobayashi, et al. 2002; Park, et al. 2007; Hall, et al. 2008). Concerning this issue, Yan and collaborators (Yan, et al. 2007) found evidence that hyperthermia induces Toll-like receptor expression and TLR signaling-mediated activation of the NF- $\kappa$ B and MAPK (mitogen-activated protein kinase) pathways, resulting in increased synthesis of pro- and anti-inflammatory cytokines. These and other similar data (Zhao, et al. 2007) indicate that heat stress (such as fever or localized temperature increase in an inflamed area) may modulate immune responses by the TLR pathway, and provide a potential link to *RIPK2* expression changes under temperature variation.

## Final Remarks and Conclusions

To the best of our knowledge, this is the first report showing splicing imbalances of the *RIPK2* gene. In brief, our results showed that, unlike variant 1, variant 2 is regulated by temperature. Both are co-expressed in normal tissues, but variant 2 has significantly increased levels in tumors versus surgical margins, as determined by quantitative PCR (qPCR) assays in oral and larynx carcinoma and normal samples. At the protein level, isoform 1 was apparently less expressed in tumors than in margins and, although truncated transcript 2 has coding potential, we found no direct evidence that it is translated in isoform 2 in the tissues and cell lines analyzed.

Considering that the same transcript, potentially encoding a truncated kinase domain, was conserved for millions of years, the human variant 2 may have a functional significance. The finding that transcript 2 and isoform 1 have opposite expression profiles is compatible with a regulatory relationship modulated by a dominant-negative mechanism, in a similar way to the regulation performed by the short RIP-1, another kinase of the RIP family. Even without clarifying this issue, the present study raises many questions about RNA biology that may stimulate further functional investigation of the molecular mechanisms underlying *RIPK2* splicing regulation and their links to physiological and environmental changes.

## Materials and Methods

### In-silico Splicing Analysis

An analysis of human *RIPK2* transcripts was performed using the Basic Local Alignment Search, Global Alignment and C-D (Conserved Domains) Tools (BLAST) (Altschul, et al. 1990), BLAST-like Alignment Tool (BLAT) (Kent 2002), Gene database (NCBI) (Benson, et al. 2013), UniProt (2010), gnomAD (Karczewski, et al. 2020), The Genotype-Tissue Expression (2013), and The Human Protein Atlas (Uhlen, et al. 2005). The sequences analyzed were: (a) the full-length variant 1 (NM\_003821.6), (b) variant 2 (NM\_001375360.1), (c) the predicted variant X1 (XM\_011517357.3) and (d) the sequence identified by us (AY562996.1).

We also investigated *RIPK2* variant 2 in twelve mammals of all orders of the supraorder Euarchontoglires (also called Supraprimates), using the transcript and protein sequences reported in [supplementary table S1, Supplementary Material](#) online and [supplementary File S1, Supplementary Material](#) online and the same tools cited above. *Canis lupus familiaris* (dog, order Carnivora) was used as an outgroup. Order, family, genus, species, and common name of mammals analyzed in the present study are presented in [Table 2](#).

Transcript and protein sequences included reviewed and provisional ones (NM, NR and NP) and the ones predicted by automated computational analysis and supported by mRNA or EST evidence (XM and XP).

BLAST Global Alignment Tool was used to search the identity percentage of exons 1-3 sequences analyzed by the present study compared with the consensus NM\_003821.6 transcript (*Homo sapiens*). This tool also provided the amino acid sequence percentage identity when the consensus isoform from each mammal was compared with the truncated isoform presenting TIS in exon 3 (from the same mammal). The identity of the kinase domain was evaluated by the BLAST C-D Tool. Alignments were obtained using the NCBI sequences and the more recent UCSC genome assembly of each mammal, except for *Lepus* and *Tupaia*. *Lepus* UCSC genome assembly is not available and *Tupaia*



**Table 2**

Mammal species of superorder euarchontoglires (supraprimates) and superorder Laurasiatheria analyzed in the present study

Superorder Euarchontoglires (Supraprimates)			
Order	Family	Genus specie	Common Name
Primates	Hominidae	<i>Homo sapiens</i>	human
		<i>Pan troglodytes</i>	chimpanzee
		<i>Gorilla gorilla gorilla</i>	gorilla
		<i>Pongo pygmaeus</i>	orangutan
		<i>Nomascus leucogenys</i>	gibbon
	Hylobatidae		
	Cercopithecidae	<i>Macaca mulatta</i>	Rhesus macaque
Dermoptera	Cynocephalidae	<i>Galeopterus variegatus</i>	Sunda flying lemur
Lagomorpha	Leporidae	<i>Lepus europaeus</i>	hare
	Ochotonidae	<i>Ochotona curzoniae</i>	pika
Rodentia	Muridae	<i>Mus musculus</i>	House mouse
		<i>Rattus norvegicus</i>	Norway rat
		<i>Tupaia chinensis</i>	Tree shrew
Outgroup Superorder Laurasiatheria			
Order	Family	Genus specie	Common Name
Carnivora	Canidae	<i>Canis lupus familiaris</i>	dog

UCSC assembly (2006, Broad/tupBel1) showed many gaps and inconclusive results (supplementary File S1, Supplementary Material online, pages 74 to 80). Thus, the alignments were performed using the BLAST Global Alignment Tool and two genome shotgun sequences: NC\_084830.1 (*Lepus europaeus* isolate LE1 chromosome 4, mLeptim1.pri, region complement 53495737 to 53525433), and NW\_006160059.1 (*Tupaia chinensis* unplaced genomic scaffold, TupChi\_1.0 Scaffold000547\_1, region 1480814-1531425).

Multiz Alignments of 100 Vertebrates; 30 mammals conservation by PhastCons (27 primates); Mammals Multiz Alignment & Conservation (27 primates) and 470 mammals Basewise Conservation by PhyloP were obtained by the UCSC browser using the genome assembly Dec. 2013 (GRCh38/hg38).

In addition, the *RIPK2* gene was interrogated for novel splice isoforms using The Cancer Genome Atlas (TCGA) Program (Weinstein, et al. 2013). The TCGA (The Cancer Genome Atlas) SpliceSeq tool (Ryan, et al. 2012) was also used to confirm the exons involved in AS events, although with different numbering.

### Samples and Cell Lines

Nine samples of normal human tissues obtained at autopsy (brain, testis, heart, lung, stomach, kidney, larynx, liver and tongue samples) and 16 matched tumor/resection margin samples of oral squamous cell carcinoma (OSCC) were used to evaluate the expression of *RIPK2* transcripts. RIP-2 protein levels were investigated in 17 matched tumor (T)/surgical margins (M) from oral (T1/M1—T9/M9 samples) and laryngeal (T10/M10—T17/M17 samples) SCCs.

Patients were recruited by the Head and Neck Cancer Research Consortium (GENCAPO) between 2006 and 2016 at the Clinics Hospital of the School of Medicine of University of São Paulo, Heliópolis Hospital, Arnaldo Vieira de Carvalho Cancer Institute (São Paulo, SP), Clinics Hospital of University of São Paulo (Ribeirão Preto, SP), and University of Vale do Paraíba, (São José dos Campos, SP). All cancer patients received no preoperative radiation or chemotherapy and were diagnosed with clinically and histologically confirmed primary squamous cell carcinoma of the head and neck (subsites C02 = other and unspecified parts of tongue; C04 = floor of mouth; C32 = larynx; according to the International Classification of Diseases, 10th revision—ICD-10). The tumors were classified by the TNM system according to tumor size (T), lymph node spread (N), and distant metastasis (M). Immediately after their collection, the samples were assigned a laboratory code to maintain confidentiality. Analysis of hematoxylin and eosin-stained sections indicated that each tumor sample contained at least 70% tumor cells and the surgical margins were tumor-free.

A pilot study was conducted on three cell lines to select the one(s) showing good performance in stress experiments: the FaDu cell line (HTB-43, American Type Culture Collection/ATCC), derived from an SCC of the hypopharynx; the SiHa cell line (HTB-35, ATCC), derived from an SCC of the cervix; and the HEP-2 cell line (CCL-23, ATCC), originally established from a laryngeal carcinoma. The identity of the cells was confirmed by cell line authentication (STR profiling).

The cell lines were cultured in Eagle's Minimum Essential Medium (MEM, Cultilab) supplemented with 10% fetal bovine serum (FBS, Cultilab), 10 mM nonessential amino acids (M7145, Sigma—Aldrich), 2 mM L-glutamine (Cultilab),



1 mM sodium pyruvate (P5280, Sigma–Aldrich), 1.5 g/L sodium bicarbonate (S5761, Sigma–Aldrich), penicillin (100 units/mL) and streptomycin (90 µg/mL) (Cultilab) at 37 °C in a humidified atmosphere with 5% CO<sub>2</sub>.

*RIPK2* transcripts and proteins were analyzed by PCR and Western blot assays, respectively. Proteins from the BHK-21 cell line (C-13, CCL-10, fibroblasts from hamster kidneys, ATCC) were used as an external reference in Western blot assays.

The study protocol was approved by the National Committee of Ethics in Research (CONEP 1763/05, 18/05/12/2005, and CONEP 128/12, 02/03/2012), and informed consent was obtained from all patients enrolled.

### Temperature and Acid Stresses

Replicates of FaDu, SiHa and Hep-2 cells were grown to 80% to 90% confluence, and the cell cycle was synchronized in serum-free medium for 24 h. The cells were incubated in serum-containing medium during the stress experiments. For temperature stress, cells were maintained at 40 °C, 17 °C or 5 °C for 3 h. For acid stress, cell lines were grown in a humidified atmosphere with 10% CO<sub>2</sub> at 37 °C for 24 or 72 h. Four or eight replicates were assayed for each condition. Six control replicates were also cultured in medium with FBS at 37 °C and 5% CO<sub>2</sub>. Immediately after treatments, the cells were lysed by adding TRIzol (15596026, Thermo Fisher Scientific) and stored at –80 °C until RNA and protein extraction.

### RNA Extraction and cDNA Synthesis

RNA from tissue samples and cell lines was obtained following the TRIzol protocol. The integrity of the RNA was confirmed by gel electrophoresis, and the purity and concentration were determined using a NanoDrop ND-1000 spectrophotometer (Thermo Fisher Scientific). One microgram of total RNA was converted to cDNA using the High-Capacity cDNA Reverse Transcription kit (4368813, Applied Biosystem) according to the manufacturer's instructions.

### Detection of *RIPK2* Transcripts by Conventional Polymerase Chain Reaction (PCR)

The levels of *RIPK2* transcripts were evaluated in cell lines, normal tissues obtained at autopsy, and matched pairs of tumor and resection margin samples using the following primer sequences: CGCCTCTGGCACTGTGTCGT-3' (*RIPK2* forward primer F) and 5'-CGTGACTGTGAGAGGGACAT-3' (*RIPK2* reverse primer R). The PCR primers for the endogenous control gene *GAPDH* were *GAPDH* forward (5'-ACCCACTCCTCCACCTTTGA-3') and *GAPDH* reverse (5'-CTGTTGCTGTAGCCAAATTCGT-3'). Conventional PCR was carried out in a total volume of 25 µL containing 1X PCR buffer, 1 mM MgCl<sub>2</sub>, 2 µM of each *RIPK2* primer, 2 µM *GAPDH* primers, 5 mM dNTP mix, 1 U of Taq DNA

polymerase (EP0402, Thermo Fisher Scientific) and 50 ng of cDNA. After a denaturation step at 94 °C, amplification was performed in a 9700 GeneAmp PCR System (Applied Biosystems). The PCR program consisted of 35 cycles of denaturation at 94 °C for 50 s, annealing at 58 °C for 40 s, and extension at 72 °C for 50 s, followed by one final cycle at 72 °C for 10 min. The expected lengths for PCR amplicons were 101 bp for *GAPDH* and 456 and 302 bp for *RIPK2* transcripts 1 and 2, respectively. The amplicons were separated on 2% agarose gels or 7.5% polyacrylamide gel and sequenced in both directions after being isolated from the gels. The sequences were analyzed using a BLAST similarity search against the nonredundant database available from NCBI (Johnson, et al. 2008).

The pilot study conducted on FaDu, SiHa, and Hep-2 cells showed that only FaDu cells exposed to temperature stress exhibited a variable expression pattern of *RIPK2* transcripts. FaDu was thus selected for RT–PCR and Western blot assays.

### Evaluation of *RIPK2* Transcripts by Relative Quantification Using RT–qPCR

The expression of *RIPK2* transcripts was investigated by qPCR assays in 16 matched pairs of oral tumor and resection margin samples and in eight replicates of FaDu cells following stress treatment. As a control for the heat/cold experiment, the RNA expression of the *HSPA1A* gene (heat-shock protein family A (Hsp70) member 1A) was also investigated. Reactions were performed in triplicate using an ABI Prism 7500 Sequence Detection System (Applied Biosystems). The primers were manually designed and optimized for RT–qPCR using basic parameters for PCR primer design. The final sequences were 19 to 24 bp long, with 30% to 70% GC content and producing short amplicon sizes (66 to 104 bp), as follows: *RIPK2* transcript 1 forward 5'-AGAAGCTGAAATTTACACAAAGC-3' and reverse 5'-CCATTTGGCATGTATTCAGTAAC-3'; *RIPK2* transcript 2 forward 5'-TGCTCGACAGAAAAGTGAATATC-3' and reverse 5'-AAGGAGGAGTCATATTGTGCAG-3'; *GAPDH* forward 5'-ACCCACTCCTCCACCTTTGA-3' and reverse 5'-CTGTTGCTGTAGCCAAATTCGT-3'; *TUBA1C* forward 5'-TCAACACCTTCTTCAGTGAAACG-3' and reverse 5'-AGTGCCAGTGCGAACTTCATC-3'; *ACTB* forward 5'-GGCA CCCAGCACAATGAAG-3' and reverse 5'-CCGATCCACAC GGAGTACTTG-3'; and *HSPA1A* forward 5'-CCGAGAAGG ACGAGTTTGAG –3' and reverse 5'-CTGGTACAGTCCGCT GATGA-3'.

All primers were purchased from Invitrogen (Thermo Fisher Scientific). Briefly, reactions were carried out in a total volume of 20 µL with 10 µL of SYBR Green PCR Master Mix (Applied Biosystem), 250 nM of each primer and 20 ng of cDNA. The PCR conditions were 50 °C for 2 min and 95 °C for 10 min followed by 40 cycles of 95 °C for 15 s, 58 °C for

10 s, and 60 °C for 1 min. Following qPCR, a dissociation curve was generated to confirm that a single gene product was generated. Three reference genes were selected by the geNorm algorithm (Vandesompele, et al. 2002): *ACTB* for tumor/margin samples and *GAPDH* or *TUBA1C* for heat/cold stress assays. The relative expression ratio (fold-change) of the target genes was calculated according to Pfaffl (Pfaffl 2001). Statistical analysis was carried out by two-tailed unpaired *t* test using GraphPad Prism (GraphPad Software, Inc.). Values were log2 transformed, and those below –1 indicated downregulation in gene expression, while values above 1 represented upregulation. Significant differences were defined by  $P < 0.05$ .

### Protein Extraction and Western Blot Analysis

Protein fractions from the tissue samples and FaDu cell line were obtained after RNA extraction by TRIzol, as described previously by our group (Polachini, et al. 2012). The protein concentrations were determined using a Pierce BCA Protein Assay Kit (Thermo Fisher Scientific).

The anti-RIP-2 primary antibodies used were as follows: (a) a rabbit polyclonal antibody (ab8428, Abcam, immunogenic peptide corresponding to amino acids 11/30 of human RIP-2, N-terminal domain, diluted 2:1000 or 3:1000); (b) a mouse monoclonal antibody (ab57954, Abcam, immunogenic peptide corresponding to amino acids 431 to 541, C-terminal domain, used at a concentration of 2 to 4 µg/mL); (c) a goat polyclonal (C-19) antibody (sc-8611, Santa Cruz Biotechnology, Inc., immunogenic peptide corresponding to the C-terminal domain, diluted 1:100 to 1:200); (d) a rabbit monoclonal antibody (D10B11) (#4142, Cell Signaling Technology/CST, immunogenic peptide near the C-terminal domain, diluted 1:10000. The antibodies against housekeeping proteins were (a) a rabbit monoclonal anti-COX IV (3E11) antibody (#4850, CST, diluted 1:1000); (b) a rabbit monoclonal anti-β-tubulin (9F3) antibody (#2128, CST, diluted 1:1000); (c) a rabbit monoclonal anti-histone H3 (D1H2) XP® antibody (#4499, CST, diluted 1:1000); (d) a rabbit monoclonal anti-GAPDH (D16H11) XP® antibody (#5174, CST, diluted 1:1000); (e) a mouse monoclonal anti-β-actin antibody (A5441, Sigma-Aldrich, diluted 1:5000).

In brief, protein samples (10 to 30 µg) were separated by SDS–PAGE (12% resolving gel with 5% stacking gel) at 130 V for 70 min in denaturing conditions. The molecular weight ladder used was the PageRuler Prestained Protein Ladder (#26616, Thermo Fisher Scientific). The proteins were then transferred electrophoretically (162.5 mA per blot for 70 min; Mini-Protean 3 Cell System, Bio-Rad Laboratories, Inc.) to polyvinylidene fluoride (PVDF) membranes (IPVH00010, Immobilon-P, Merck Millipore) in transfer buffer (25 mM Tris, 0.2 M glycine, 20% v/v methanol; Merck Millipore). After blocking, the membranes were

incubated with primary antibodies overnight at 4 °C and then with HRP (horseradish peroxidase)-conjugated secondary antibodies (074 to 1506, 074-1806, KPL, Kirkegaard & Perry Laboratories, Inc.). The immunoreactive bands were detected using a chemiluminescence detection kit (Amersham ECL Select Western Blotting Detection Reagent, RPN2235) according to the manufacturer's protocol, and the proteins were visualized using a Fusion FX5 system (Vilber Lourmat). The PVDF membranes were also subjected to chromogenic staining using a WesternBreeze Chromogenic Kit (Invitrogen, Thermo Fisher Scientific). The blots were then scanned and analyzed (Gel Logic HP 2200 imaging system, Carestream Health Inc./Kodak Health Group). Different exposure times were tested for band development (1 to 30 min or 5 to 60 s in chromogenic or chemiluminescent assays, respectively).

### MS and Protein Identification

Protein bands at ~41 to 45 kDa were excised manually from Western blot membranes and one-dimensional electrophoresis gels, reduced, alkylated and submitted to in-gel digestion with trypsin, as described previously by our group (Polachini, et al. 2012). In brief, an aliquot of the peptide mixture was separated using a C18 column RP-nanoUPLC (nanoAcquity, Waters Corp., Milford) coupled with a Q-ToF Ultima mass spectrometer (Waters) with nano-electrospray source. The gradient was acetonitrile in formic acid over 45 min. The instrument was operated in the “top three” mode, in which one MS spectrum is acquired followed by MS/MS of the top three most-intense peaks detected. The spectra were analyzed using the MassLynx software version 4.1 (Waters) and the raw data files were converted to a peak list format (mgf) by the Mascot Distiller software, version 2.2.1.0, 2008 (Matrix Science Ltd., London).

### Protein Sequence Alignment and Homology Modeling Procedures

Homology modeling of RIP-2 isoforms 1 and 2 was carried out using MODELLER software, which performs modeling by satisfying spatial restraints (Sali and Blundell 1990). Six homologs with structures available in the Protein Data Bank (codes: 2GSF, 1JPA, 1K2P, 1U59, 1UWH, 2EVA) used as templates were selected through a nonredundant BLASTp search (Johnson, et al. 2008). Two putative conserved domains with statistical significance were detected: TyrKc and S\_TKc, which correspond to the catalytic domains of tyrosine and serine/threonine protein kinases, respectively, and include the leucine L10-threonine T296 sequence. These six templates share sequence identities of 27.1% (Eph receptor tyrosine kinase, PDB code: 1JPA) to 30% (transforming growth factor-β [TGF-β]-activated kinase 1—TAK1, PDB code: 2EVA) with RIP-2. Analyses were performed using pairwise alignments via the AMPS

(Alignment of Multiple Protein Sequences) package (Barton and Sternberg 1987). Prior to modeling, a final multiple alignment was obtained by analyzing the superposition of the six structures regarding the  $\alpha$ -carbons of the residues using the INSIGHT II program, version 2005 (Accelrys, Inc.), which allowed refinement of the previous alignment obtained from the AMPS MULTALIGN module. The secondary structure information in the template sequence was incorporated into this previous alignment using the MULTALIGN module of the AMPS package, with the restriction that all insertions and deletions were limited to regions outside the common core of  $\alpha$ -helices and  $\beta$ -sheets. A gap penalty of 1000 was fixed to any deletion or insertion inside a secondary structure element. The alignment obtained was edited, investigating and considering the aligned residues, which were close in space, as visualized in the structural superposition. This procedure resulted in a final alignment that was different from the one based on the Dayhoff matrix (PAM 250) used in AMPS.

The NetPhosK 1.0 server (Blom, et al. 2004) was used for phosphorylation site analyses. The algorithm produces neural network predictions of kinase-specific eukaryotic protein phosphorylation sites. Currently, NetPhosK covers the following kinases: PKA, PKC, PKG, CKII, Cdc2, CaM-II, ATM, DNA PK, Cdk5, p38 MAPK, GSK3, CKI, PKB, RSK, INSR, EGFR, and Src.

## Supplementary Material

Supplementary material is available at *Genome Biology and Evolution* online.

## Acknowledgments

The authors are grateful to Mauro Golin for artwork preparation, and to GENCAPO (Head and Neck Genome Project) team for the valuable discussions that motivated the present study. The authors also acknowledge the Mass Spectrometry Laboratory at Brazilian Biosciences National Laboratory (LNBio), CNPEM/ABTLuS, Campinas, Brazil, for their support with the mass spectrometry analysis.

## Author Contributions

U.M.M.V. participated in the design of the study, performed stress and gene expression experiments, and in-silico splicing analysis; B.R.C. and C.B.S. performed stress and gene expression experiments; G.M.P. performed MS and Western blot experiments; T.H. performed the analysis of the data and preparation of the manuscript; T.B.C. participated in the literature review and interpretation of the data; C.H.T.P.S. and O.A.F performed homology modeling procedures; R.V.M.L. carried out the analysis of the demographic data for sample selection; E.D-N and F.D. evaluated and interpreted the results; P.S. evaluated and interpreted

the results and participated in writing the manuscript; E.H.T. conceived and coordinated the design of the study, evaluated and interpreted the results, wrote the manuscript and supervised all the process. All authors critically read the manuscript, checked the accuracy of the data, and approved the version to be published.

## Funding Statement

This work was supported by the Fundação de Amparo à Pesquisa do Estado de São Paulo/FAPESP (grant number 10/51168-0 to E.H.T.; fellowships 03/07802-3 to U.M.M.V., 11/23353-0 G.M.P., 12/06048-2 to B.R.C., 19/07293-0 to T.B.C.); and Conselho Nacional de Desenvolvimento Científico e Tecnológico/CNPq (grant numbers 308904/2014-1 and 306216/2010-8 to E.H.T.; fellowships 140107/2015-0 to A.C.B.S., 307327/2018-3 to E.H.T.).

## Conflicts of Interest

The authors declare no competing interests.

## Data Availability

The data underlying this article are available in the article and in its online supplementary material.

## Literature Cited

- Adjirackor NA, Harvey KE, Harvey SC. Eukaryotic response to hypothermia in relation to integrated stress responses. *Cell Stress Chaperones*. 2020;25(6):833–846. <https://doi.org/10.1007/s12192-020-01135-8>.
- Al-Fageeh MB, Smales CM. Control and regulation of the cellular responses to cold shock: the responses in yeast and mammalian systems. *Biochem J*. 2006;397(2):247–259. <https://doi.org/10.1042/BJ20060166>.
- Altschul SF, Gish W, Miller W, Myers EW, Lipman DJ. Basic local alignment search tool. *J Mol Biol*. 1990;215(3):403–410. [https://doi.org/10.1016/S0022-2836\(05\)80360-2](https://doi.org/10.1016/S0022-2836(05)80360-2).
- Andreev DE, Arnold M, Kiniry SJ, Loughran G, Michel AM, Rachinskii D, Baranov PV. TASEP modelling provides a parsimonious explanation for the ability of a single uORF to derepress translation during the integrated stress response. *Elife*. 2018;7:e32563. <https://doi.org/10.7554/eLife.32563>.
- Baralle M, Romano M. Age-Related alternative splicing: driver or passenger in the aging process? *Cells*. 2023;13:12. <https://doi.org/10.3390/cells12242819>.
- Barton GJ, Sternberg MJ. A strategy for the rapid multiple alignment of protein sequences. Confidence levels from tertiary structure comparisons. *J Mol Biol*. 1987;198(2):327–337. [https://doi.org/10.1016/0022-2836\(87\)90316-0](https://doi.org/10.1016/0022-2836(87)90316-0).
- Baudier J, Gentil BJ. The S100B protein and partners in adipocyte response to cold stress and adaptive thermogenesis: facts, hypotheses, and perspectives. *Biomolecules*. 2020;10(6):843. <https://doi.org/10.3390/biom10060843>.
- Benson DA, Cavanaugh M, Clark K, Karsch-Mizrachi I, Lipman DJ, Ostell J, Sayers EW. GenBank. *Nucleic Acids Res*. 2013;41(Database issue):D36–D42. <https://doi.org/10.1093/nar/gks1195>.

- Bjorklund SS, Panda A, Kumar S, Seiler M, Robinson D, Gheeya J, Yao M, Alnæs GIG, Toppmeyer D, Riis M, et al. Widespread alternative exon usage in clinically distinct subtypes of invasive ductal carcinoma. *Sci Rep*. 2017;7(1):5568. <https://doi.org/10.1038/s41598-017-05537-0>.
- Blencowe BJ. The relationship between alternative splicing and proteomic complexity. *Trends Biochem Sci*. 2017;42(6):407–408. <https://doi.org/10.1016/j.tibs.2017.04.001>.
- Blom N, Sicheritz-Ponten T, Gupta R, Gammeltoft S, Brunak S. Prediction of post-translational glycosylation and phosphorylation of proteins from the amino acid sequence. *Proteomics*. 2004;4(6):1633–1649. <https://doi.org/10.1002/pmic.200300771>.
- Bowling A, Eastman A, Merlo C, Lin G, West N, Patel S, Cutting G, Sharma N. Downstream alternate start site allows N-terminal nonsense variants to escape NMD and results in functional recovery by readthrough and modulator combination. *J Pers Med*. 2022;12(9):1448. <https://doi.org/10.3390/jpm12091448>.
- Brady LK, Wang H, Radens CM, Bi Y, Radovich M, Maity A, Ivan C, Ivan M, Barash Y, Koumenis C. Transcriptome analysis of hypoxic cancer cells uncovers internal retention in EIF2B5 as a mechanism to inhibit translation. *PLoS Biol*. 2017;15(9):e2002623. <https://doi.org/10.1371/journal.pbio.2002623>.
- Callow MG, Watanabe C, Wickliffe KE, Bainer R, Kummerfield S, Weng J, Cuellar T, Janakiraman V, Chen H, Chih B, et al. CRISPR whole-genome screening identifies new necroptosis regulators and RIPK1 alternative splicing. *Cell Death Dis*. 2018;9(3):261. <https://doi.org/10.1038/s41419-018-0301-y>.
- Chirieleison SM, Kertesz SB, Abbott DW. Synthetic biology reveals the uniqueness of the RIP kinase domain. *J Immunol*. 2016;196(10):4291–4297. <https://doi.org/10.4049/jimmunol.1502631>.
- Cote GJ, Zhu W, Thomas A, Martin E, Murad F, Sharina IG. Hydrogen peroxide alters splicing of soluble guanylyl cyclase and selectively modulates expression of splicing regulators in human cancer cells. *PLoS One*. 2012;7(7):e41099. <https://doi.org/10.1371/journal.pone.0041099>.
- Cui J, Sinoway LI. Cardiovascular responses to heat stress in chronic heart failure. *Curr Heart Fail Rep*. 2014;11(2):139–145. <https://doi.org/10.1007/s11897-014-0191-y>.
- Cuny GD, Degterev A. RIPK protein kinase family: atypical lives of typical kinases. *Semin Cell Dev Biol*. 2021;109:96–105. <https://doi.org/10.1016/j.semcdb.2020.06.014>.
- Dasgupta M, Agarwal MK, Varley P, Lu T, Stark GR, Kandel ES. Transposon-based mutagenesis identifies short RIP1 as an activator of NFκB. *Cell Cycle*. 2008;7(14):2249–2256. <https://doi.org/10.4161/cc.7.14.6310>.
- Dominguez CE, Cunningham D, Venkataramany AS, Chandler DS. Heat increases full-length SMN splicing: promise for splice-augmenting therapies for SMA. *Hum Genet*. 2022;141(2):239–256. <https://doi.org/10.1007/s00439-021-02408-7>.
- Dorsch M, Wang A, Cheng H, Lu C, Bielecki A, Charron K, Clauser K, Ren H, Polakiewicz RD, Parsons T, et al. Identification of a regulatory autophosphorylation site in the serine-threonine kinase RIP2. *Cell Signal*. 2006;18(12):2223–2229. <https://doi.org/10.1016/j.cellsig.2006.05.005>.
- Elias AP, Dias S. Microenvironment changes (in pH) affect VEGF alternative splicing. *Cancer Microenviron*. 2008;1(1):131–139. <https://doi.org/10.1007/s12307-008-0013-4>.
- Eng VV, Wemyss MA, Pearson JS. The diverse roles of RIP kinases in host-pathogen interactions. *Semin Cell Dev Biol*. 2021;109:125–143. <https://doi.org/10.1016/j.semcdb.2020.08.005>.
- Fan Y, Huang Z-Y, Cao C-C, Chen C-S, Chen Y-X, Fan D-D, He J, Hou H-L, Hu L, Hu X-T, et al. Genome of the Chinese tree shrew. *Nat Commun*. 2013;4(1):1426. <https://doi.org/10.1038/ncomms2416>.
- Farashahi Yazd E, Rafiee MR, Soleimani M, Tavallaei M, Salmani MK, Mowla SJ. OCT4B1, a novel spliced variant of OCT4, generates a stable truncated protein with a potential role in stress response. *Cancer Lett*. 2011;309(2):170–175. <https://doi.org/10.1016/j.canlet.2011.05.027>.
- Farashi S, Sharifi E. Stem cell behavior at hypothermia: a review article. *Curr Stem Cell Res Ther*. 2021;16(6):718–729. <https://doi.org/10.2174/1574888X16666201229124842>.
- Fox-Walsh KL, Dou Y, Lam BJ, Hung SP, Baldi PF, Hertel KJ. The architecture of pre-mRNAs affects mechanisms of splice-site pairing. *Proc Natl Acad Sci U S A*. 2005;102(45):16176–16181. <https://doi.org/10.1073/pnas.0508489102>.
- Gambino TJ, Williams SP, Caesar C, Resnick D, Nowell CJ, Farnsworth RH, Achen MG, Stacker SA, Karnezis T. A three-dimensional lymphatic endothelial cell tube formation assay to identify novel kinases involved in lymphatic vessel remodeling. *Assay Drug Dev Technol*. 2017;15(1):30–43. <https://doi.org/10.1089/adt.2016.764>.
- Gelfman S, Burstein D, Penn O, Savchenko A, Amit M, Schwartz S, Pupko T, Ast G. Changes in exon-intron structure during vertebrate evolution affect the splicing pattern of exons. *Genome Res*. 2012;22(1):35–50. <https://doi.org/10.1101/gr.119834.110>.
- Gemignani F, Sazani P, Morcos P, Kole R. Temperature-dependent splicing of beta-globin pre-mRNA. *Nucleic Acids Res*. 2002;30(21):4592–4598. <https://doi.org/10.1093/nar/gkf607>.
- Gomez Acuna LI, Fiszbein A, Allo M, Schor IE, Kornblihtt AR. Connections between chromatin signatures and splicing. *Wiley Interdiscip Rev RNA*. 2013;4(1):77–91. <https://doi.org/10.1002/wrna.1142>.
- Goncharov T, Hedayati S, Mulvihill MM, Izrael-Tomasevic A, Zobel K, Jeet S, Fedorova AV, Eidenschen C, deVoss J, Yu K, et al. Disruption of XIAP-RIP2 association blocks NOD2-mediated inflammatory signaling. *Mol Cell*. 2018;69(4):551–565.e7. <https://doi.org/10.1016/j.molcel.2018.01.016>.
- Gotthardt M, Badillo-Lisakowski V, Parikh VN, Ashley E, Furtado M, Carmo-Fonseca M, Schudy S, Meder B, Grosch M, Steinmetz L, et al. Cardiac splicing as a diagnostic and therapeutic target. *Nat Rev Cardiol*. 2023;20(8):517–530. <https://doi.org/10.1038/s41569-022-00828-0>.
- Gracio F, Burford B, Gazinska P, Mera A, Mohd Noor A, Marra P, Gillett C, Grigoriadis A, Pinder S, Tutt A, et al. Splicing imbalances in basal-like breast cancer underpin perturbation of cell surface and oncogenic pathways and are associated with patients' survival. *Sci Rep*. 2017;7(1):40177. <https://doi.org/10.1038/srep40177>.
- Greenbaum D, Colangelo C, Williams K, Gerstein M. Comparing protein abundance and mRNA expression levels on a genomic scale. *Genome Biol*. 2003;4(9):117. <https://doi.org/10.1186/gb-2003-4-9-117>.
- Gross JH. *Mass Spectrometry. A Textbook*. 2017. Springer: Springer Cham. <https://doi.org/10.1007/978-3-319-54398-7>.
- GTEx Consortium. 2013. The genotype-tissue expression (GTEx) project. *Nat Genet* 45(6): 580–585. <https://doi.org/10.1038/ng.2653>.
- Gutierrez-Arcelus M, Ongen H, Lappalainen T, Montgomery SB, Buil A, Yurovsky A, Bryois J, Padioulet I, Romano L, Planchon A, et al. Tissue-specific effects of genetic and epigenetic variation on gene regulation and splicing. *PLoS Genet*. 2015;11(1):e1004958. <https://doi.org/10.1371/journal.pgen.1004958>.
- Hall HT, Wilhelm MT, Saibil SD, Mak TW, Flavell RA, Ohashi PS. RIP2 contributes to nod signaling but is not essential for T cell proliferation, T helper differentiation or TLR responses. *Eur J Immunol*. 2008;38(1):64–72. <https://doi.org/10.1002/eji.200737393>.
- Han NC, Kelly P, Ibba M. Translational quality control and reprogramming during stress adaptation. *Exp Cell Res*. 2020;394(2):112161. <https://doi.org/10.1016/j.yexcr.2020.112161>.



- He S, Wang X. RIP kinases as modulators of inflammation and immunity. *Nat Immunol.* 2018;19(9):912–922. <https://doi.org/10.1038/s41590-018-0188-x>.
- Hernandez G, Osnaya VG, Perez-Martinez X. Conservation and variability of the AUG initiation Codon context in eukaryotes. *Trends Biochem Sci.* 2019;44(12):1009–1021. <https://doi.org/10.1016/j.tibs.2019.07.001>.
- Horii Y, Shiina T, Uehara S, Nomura K, Shimaoka H, Horii K, Shimizu Y. Hypothermia induces changes in the alternative splicing pattern of cold-inducible RNA-binding protein transcripts in a non-hibernator, the mouse. *Biomed Res.* 2019;40(4):153–161. <https://doi.org/10.2220/biomedres.40.153>.
- Hu Z, Liang MC, Soong TW. Alternative splicing of L-type  $\text{Ca}^{2+}$  channels: implications in cardiovascular diseases. *Genes (Basel).* 2017;8(12):344. <https://doi.org/10.3390/genes8120344>.
- Inohara N, del Peso L, Koseki T, Chen S, Nunez G. RICK, a novel protein kinase containing a caspase recruitment domain, interacts with CLARP and regulates CD95-mediated apoptosis. *J Biol Chem.* 1998;273(20):12296–12300. <https://doi.org/10.1074/jbc.273.20.12296>.
- Inohara N, Nunez G. NODs: intracellular proteins involved in inflammation and apoptosis. *Nat Rev Immunol.* 2003;3(5):371–382. <https://doi.org/10.1038/nri1086>.
- Jobbins AM, Yu S, Paterson HAB, Maude H, Kefala-Stavridi A, Speck C, Cebola I, Vernia S. Pre-RNA splicing in metabolic homeostasis and liver disease. *Trends Endocrinol Metab.* 2023;34(12):823–837. <https://doi.org/10.1016/j.tem.2023.08.007>.
- Johnson M, Zaretskaya I, Raytselis Y, Merezukh Y, McGinnis S, Madden TL. NCBI BLAST: a better web interface. *Nucleic Acids Res.* 2008;36(Web Server):W5–W9. <https://doi.org/10.1093/nar/gkn201>.
- Kahles A, Lehmann K-V, Toussaint NC, Hüser M, Stark SG, Sachsenberg T, Stegle O, Kohlbacher O, Sander C, Rätsch G, et al. Comprehensive analysis of alternative splicing across tumors from 8,705 patients. *Cancer Cell.* 2018;34(2):211–224.e6. <https://doi.org/10.1016/j.ccell.2018.07.001>.
- Karczewski KJ, Francioli LC, Tiao G, Cummings BB, Alföldi J, Wang Q, Collins RL, Laricchia KM, Ganna A, Birnbaum DP, et al. The mutational constraint spectrum quantified from variation in 141,456 humans. *Nature.* 2020;581(7809):434–443. <https://doi.org/10.1038/s41586-020-2308-7>.
- Kent WJ. BLAT—the BLAST-like alignment tool. *Genome Res.* 2002;12(4):656–664. <https://doi.org/10.1101/gr.229202>.
- Kjer-Hansen P, Weatheritt RJ. The function of alternative splicing in the proteome: rewiring protein interactomes to put old functions into new contexts. *Nat Struct Mol Biol.* 2023;30(12):1844–1856. <https://doi.org/10.1038/s41594-023-01155-9>.
- Kobayashi K, Inohara N, Hernandez LD, Galán JE, Núñez G, Janeway CA, Medzhitov R, Flavell RA. RICK/rip2/CARDIAK mediates signalling for receptors of the innate and adaptive immune systems. *Nature.* 2002;416(6877):194–199. <https://doi.org/10.1038/416194a>.
- Kozak M. Point mutations define a sequence flanking the AUG initiator codon that modulates translation by eukaryotic ribosomes. *Cell.* 1986;44(2):283–292. [https://doi.org/10.1016/0092-8674\(86\)90762-2](https://doi.org/10.1016/0092-8674(86)90762-2).
- Kozak M. Effects of intercistronic length on the efficiency of reinitiation by eucaryotic ribosomes. *Mol Cell Biol.* 1987;7(10):3438–3445. <https://doi.org/10.1128/mcb.7.10.3438-3445.1987>.
- Krieg A, Correa RG, Garrison JB, Le Negrate G, Welsh K, Huang Z, Knoefel WT, Reed JC. XIAP mediates NOD signaling via interaction with RIP2. *Proc Natl Acad Sci U S A.* 2009;106(34):14524–14529. <https://doi.org/10.1073/pnas.0907131106>.
- Kuchta K, Towpik J, Biernacka A, Kutner J, Kudlicki A, Ginalska K, Rowicka M. Predicting proteome dynamics using gene expression data. *Sci Rep.* 2018;8(1):13866. <https://doi.org/10.1038/s41598-018-31752-4>.
- Kumar D, Das M, Saucedo C, Ellies LG, Kuo K, Parwal P, Kaur M, Jih L, Bandyopadhyay GK, Burton D, et al. Degradation of splicing factor SRSF3 contributes to progressive liver disease. *J Clin Invest.* 2019;129(10):4477–4491. <https://doi.org/10.1172/JCI127374>.
- Kurabi A, Lee J, Pak K, Leichtle A, Ryan AF. Essential role of the innate immune adaptor RIP2 in the response to Otitis Media. *Front Genet.* 2022;13:893085. <https://doi.org/10.3389/fgene.2022.893085>.
- Li K, Kong J, Zhang S, Zhao T, Qian W. Distance-dependent inhibition of translation initiation by downstream out-of-frame AUGs is consistent with a Brownian ratchet process of ribosome scanning. *Genome Biol.* 2022;23(1):254. <https://doi.org/10.1186/s13059-022-02829-1>.
- Liborio TN, Ferreira EN, Aquino Xavier FC, Carraro DM, Kowalski LP, Soares FA, Nunes FD. TGF1 splicing variant 8 is overexpressed in oral squamous cell carcinoma and is related to pathologic and clinical behavior. *Oral Surg Oral Med Oral Pathol Oral Radiol.* 2013;116(5):614–625. <https://doi.org/10.1016/j.oooo.2013.07.014>.
- Lopez-Mejia IC, Vautrot V, De Toledo M, Behm-Ansmant I, Bourgeois CF, Navarro CL, Osorio FG, Freije JMP, Stévenin J, De Sandre-Giovannoli A, et al. A conserved splicing mechanism of the LMNA gene controls premature aging. *Hum Mol Genet.* 2011;20(23):4540–4555. <https://doi.org/10.1093/hmg/ddr385>.
- Lu G, Du R, Feng B, Wang J, Zhang F, Pei J, Wang Y, Shang Y. A novel gene signature associated with inflammatory responses and immune Status assists in prognosis and intervention for patients with HCC. *J Inflamm Res.* 2022;15:6729–6743. <https://doi.org/10.2147/JIR.S390113>.
- Lu T, Peng H, Zhong L, Wu P, He J, Deng Z, Huang Y. The tree shrew as a model for cancer research. *Front Oncol.* 2021;11:653236. <https://doi.org/10.3389/fonc.2021.653236>.
- Mann JT, Riley BA, Baker SF. All differential on the splicing front: host alternative splicing alters the landscape of virus-host conflict. *Semin Cell Dev Biol.* 2023;146:40–56. <https://doi.org/10.1016/j.semcdb.2023.01.013>.
- Marasco LE, Kornblihtt AR. The physiology of alternative splicing. *Nat Rev Mol Cell Biol.* 2022;24(4):242–254. <https://doi.org/10.1038/s41580-022-00545-z>.
- Mauduit C, Chatelain G, Magre S, Brun G, Benahmed M, Michel D. Regulation by pH of the alternative splicing of the stem cell factor pre-mRNA in the testis. *J Biol Chem.* 1999;274(2):770–775. <https://doi.org/10.1074/jbc.274.2.770>.
- Natua S, Dhamdhare SG, Mutnuru SA, Shukla S. Interplay within tumor microenvironment orchestrates neoplastic RNA metabolism and transcriptome diversity. *Wiley Interdiscip Rev RNA.* 2022;13(2):e1676. <https://doi.org/10.1002/wrna.1676>.
- Nikom D, Zheng S. Alternative splicing in neurodegenerative disease and the promise of RNA therapies. *Nat Rev Neurosci.* 2023;24(8):457–473. <https://doi.org/10.1038/s41583-023-00717-6>.
- Noderer WL, Flockhart RJ, Bhaduri A, Diaz de Arce AJ, Zhang J, Khavari PA, Wang CL. Quantitative analysis of mammalian translation initiation sites by FACS-seq. *Mol Syst Biol.* 2014;10(8):748. <https://doi.org/10.15252/msb.20145136>.
- Palve V, Mallick S, Ghaisas G, Kannan S, Teni T. Overexpression of mcl-1L splice variant is associated with poor prognosis and chemoresistance in oral cancers. *PLoS One.* 2014;9(11):e111927. <https://doi.org/10.1371/journal.pone.0111927>.
- Pani T, Rajput K, Kar A, Dasgupta U. Alternative splicing of CERS2 promotes cell proliferation and migration in luminal B subtype breast cancer cells. *Oncoscience.* 2021;8:50–52. <https://doi.org/10.18632/oncoscience.531>.



- Park JH, Kim Y-G, McDonald C, Kanneganti T-D, Hasegawa M, Body-Malapel M, Inohara N, Núñez G. RICK/RIP2 mediates innate immune responses induced through nod1 and nod2 but not TLRs. *J Immunol.* 2007;178(4):2380–2386. <https://doi.org/10.4049/jimmunol.178.4.2380>.
- Park E, Pan Z, Zhang Z, Lin L, Xing Y. The expanding landscape of alternative splicing variation in human populations. *Am J Hum Genet.* 2018;102(1):11–26. <https://doi.org/10.1016/j.ajhg.2017.11.002>.
- Paszek A, Kardyńska M, Bagnall J, Śmieja J, Spiller DG, Widlak P, Kimmel M, Widlak W, Paszek P. Heat shock response regulates stimulus-specificity and sensitivity of the pro-inflammatory NF-kappaB signalling. *Cell Commun Signal.* 2020;18(1):77. <https://doi.org/10.1186/s12964-020-00583-0>.
- Pessa JC, Joutsen J, Sistonen L. Transcriptional reprogramming at the intersection of the heat shock response and proteostasis. *Mol Cell.* 2024;84(1):80–93. <https://doi.org/10.1016/j.molcel.2023.11.024>.
- Pfaffl MW. A new mathematical model for relative quantification in real-time RT-PCR. *Nucleic Acids Res.* 2001;29(9):e45. <https://doi.org/10.1093/nar/29.9.e45>.
- Polachini GM, Sobral LM, Mercante AMC, Paes-Leme AF., Xavier FCA, Henrique T, Guimarães DM, Vidotto A, Fukuyama EE, Góis-Filho JF, et al. Proteomic approaches identify members of cofilin pathway involved in oral tumorigenesis. *PLoS One.* 2012;7(12):e50517. <https://doi.org/10.1371/journal.pone.0050517>.
- Radhakrishnan A, Nanjappa V, Raja R, Sathe G, Chavan S, Nirujogi RS, Patil AH, Solanki H, Renuse S, Sahasrabudhe NA, et al. Dysregulation of splicing proteins in head and neck squamous cell carcinoma. *Cancer Biol Ther.* 2016;17(2):219–229. <https://doi.org/10.1080/15384047.2016.1139234>.
- Reber S, Stettler J, Filosa G, Colombo M, Jutzi D, Lenzken SC, Schweingruber C, Bruggmann R, Bachi A, Barabino SML, et al. Minor intron splicing is regulated by FUS and affected by ALS-associated FUS mutants. *EMBO J.* 2016;35(14):1504–1521. <https://doi.org/10.15252/emboj.201593791>.
- Reis EM, Ojopi EPB, Alberto FL, Rahal P, Tsukumo F, Mancini UM, Guimarães GS, Thompson GMA, Camacho C, Miracca E, et al. Large-scale transcriptome analyses reveal new genetic marker candidates of head, neck, and thyroid cancer. *Cancer Res.* 2005;65(5):1693–1699. <https://doi.org/10.1158/0008-5472.CAN-04-3506>.
- Rohani N, Hao L, Alexis MS, Joughin BA, Krismer K, Moufarrej MN, Soltis AR, Lauffenburger DA, Yaffe MB, Burge CB, et al. Acidification of tumor at stromal boundaries drives transcriptome alterations associated with aggressive phenotypes. *Cancer Res.* 2019;79(8):1952–1966. <https://doi.org/10.1158/0008-5472.CAN-18-1604>.
- Ruta V, Pagliarini V, Sette C. Coordination of RNA processing regulation by signal transduction pathways. *Biomolecules.* 2021;11(10):1475. <https://doi.org/10.3390/biom11101475>.
- Ryan MC, Cleland J, Kim R, Wong WC, Weinstein JN. SpliceSeq: a resource for analysis and visualization of RNA-Seq data on alternative splicing and its functional impacts. *Bioinformatics.* 2012;28(18):2385–2387. <https://doi.org/10.1093/bioinformatics/bts452>.
- Sali A, Blundell TL. Definition of general topological equivalence in protein structures. A procedure involving comparison of properties and relationships through simulated annealing and dynamic programming. *J Mol Biol.* 1990;212(2):403–428. [https://doi.org/10.1016/0022-2836\(90\)90134-8](https://doi.org/10.1016/0022-2836(90)90134-8).
- Sam KK, Gan CP, Yee PS, Chong CE, Lim KP, Karen-Ng LP, Chang WS, Nathan S, Rahman ZAA, Ismail SM, et al. Novel MDM2 splice variants identified from oral squamous cell carcinoma. *Oral Oncol.* 2012;48(11):1128–1135. <https://doi.org/10.1016/j.oraloncology.2012.05.016>.
- Sanada T, Tsukiyama-Kohara K, Shin-I T, Yamamoto N, Kayesh MEH, Yamane D, Takano J-I, Shioyama Y, Yasutomi Y, Ikeo K, et al. Construction of complete tupaia belangeri transcriptome database by whole-genome and comprehensive RNA sequencing. *Sci Rep.* 2019;9(1):12372. <https://doi.org/10.1038/s41598-019-48867-x>.
- Sciarrillo R, Wojtuszkiewicz A, Assaraf YG, Jansen G, Kaspers GJL, Giovannetti E, Cloos J. The role of alternative splicing in cancer: from oncogenesis to drug resistance. *Drug Resist Updat.* 2020;53:100728. <https://doi.org/10.1016/j.drug.2020.100728>.
- Scutigliani EM, Lobo-Cerna F, Mingo Barba S, Scheidegger S, Krawczyk PM. The effects of heat stress on the transcriptome of human cancer cells: a meta-analysis. *Cancers (Basel).* 2022;15(1):113. <https://doi.org/10.3390/cancers15010113>.
- Shao Y, Zhou L, Li F, Zhao L, Zhang B-L, Shao F, Chen J-W, Chen C-Y, Bi X, Zhuang X-L, et al. Phylogenomic analyses provide insights into primate evolution. *Science.* 2023;380(6648):913–924. <https://doi.org/10.1126/science.abn6919>.
- Shiina T, Shimizu Y. Temperature-Dependent alternative splicing of precursor mRNAs and its biological significance: a review focused on post-transcriptional regulation of a cold shock protein gene in hibernating mammals. *Int J Mol Sci.* 2020;21(20):7599. <https://doi.org/10.3390/ijms21207599>.
- Song X, Li X, Ge Y, Song J, Wei Q, He M, wei M, Zhang Y, Chen T, Zhao L. Alternative splicing events and function in the tumor microenvironment: new opportunities and challenges. *Int Immunopharmacol.* 2023;123:110718. <https://doi.org/10.1016/j.intimp.2023.110718>.
- Song J, Yang R, Wei R, Du Y, He P, Liu X. Pan-cancer analysis reveals RIPK2 predicts prognosis and promotes immune therapy resistance via triggering cytotoxic T lymphocytes dysfunction. *Mol Med.* 2022;28(1):47. <https://doi.org/10.1186/s10020-022-00475-8>.
- Spriggs KA, Bushell M, Willis AE. Translational regulation of gene expression during conditions of cell stress. *Mol Cell.* 2010;40(2):228–237. <https://doi.org/10.1016/j.molcel.2010.09.028>.
- Stacker SA, Williams SP, Karnezis T, Shayan R, Fox SB, Achen MG. Lymphangiogenesis and lymphatic vessel remodelling in cancer. *Nat Rev Cancer.* 2014;14(3):159–172. <https://doi.org/10.1038/nrc3677>.
- Szafrański K, Kramer M. It's a bit over, is that ok? The subtle surplus from tandem alternative splicing. *RNA Biol.* 2015;12(2):115–122. <https://doi.org/10.1080/15476286.2015.1017210>.
- Tait AS, Tarrant RD, Velez-Suberbie ML, Spencer DI, Bracewell DG. Differential response in downstream processing of CHO cells grown under mild hypothermic conditions. *Biotechnol Prog.* 2013;29(3):688–696. <https://doi.org/10.1002/btpr.1726>.
- Tang SJ, Shen H, An O, Hong H, Li J, Song Y, Han J, Tay DJT, Ng VHE, Bellido Molias F, et al. Cis- and trans-regulations of pre-mRNA splicing by RNA editing enzymes influence cancer development. *Nat Commun.* 2020;11(1):799. <https://doi.org/10.1038/s41467-020-14621-5>.
- Telonis-Scott M, Clemson AS, Johnson TK, Sgro CM. Spatial analysis of gene regulation reveals new insights into the molecular basis of upper thermal limits. *Mol Ecol.* 2014;23(24):6135–6151. <https://doi.org/10.1111/mec.13000>.
- Temaj G, Chichiarelli S, Saha S, Telkoparan-Akillilar P, Nuhii N, Hadziselimovic R, Saso L. An intricate rewiring of cancer metabolism via alternative splicing. *Biochem Pharmacol.* 2023;217:115848. <https://doi.org/10.1016/j.bcp.2023.115848>.
- Tian E, Zhou C, Quan S, Su C, Zhang G, Yu Q, Li J, Zhang J. RIPK2 inhibitors for disease therapy: current status and perspectives. *Eur J Med Chem.* 2023;259:115683. <https://doi.org/10.1016/j.ejmech.2023.115683>.
- Tigno-Aranjuez JT, Asara JM, Abbott DW. Inhibition of RIP2's tyrosine kinase activity limits NOD2-driven cytokine responses. *Genes Dev.* 2010;24(23):2666–2677. <https://doi.org/10.1101/gad.1964410>.
- Topal Y, Gyrd-Hansen M. RIPK2 NODs to XIAP and IBD. *Semin Cell Dev Biol.* 2021;109:144–150. <https://doi.org/10.1016/j.semcdb.2020.07.001>.

- Uhlen M, Björling E, Agaton C, Szgyarto CAK, Amini B, Andersen E, Andersson A-C, Angelidou P, Asplund A, Asplund C, et al. A human protein atlas for normal and cancer tissues based on antibody proteomics. *Mol Cell Proteomics*. 2005;4(12):1920–1932. <https://doi.org/10.1074/mcp.M500279-MCP200>.
- UniProt Consortium. The universal protein resource (UniProt) in 2010. *Nucleic Acids Res*. 2010;38(suppl\_1):D142–D148. <https://doi.org/10.1093/nar/gkp846>.
- Vandesompele J, De Preter K, Pattyn F, Poppe B, Van Roy N, De Paepe A, Speleman F. Accurate normalization of real-time quantitative RT-PCR data by geometric averaging of multiple internal control genes. *Genome Biol*. 2002;3(7):RESEARCH0034. <https://doi.org/10.1186/gb-2002-3-7-research0034>.
- Vostakolaei MA, Hatami-Baroogh L, Babaei G, Molavi O, Kordi S, Abdolalizadeh J. Hsp70 in cancer: a double agent in the battle between survival and death. *J Cell Physiol*. 2021;236(5):3420–3444. <https://doi.org/10.1002/jcp.30132>.
- Wang X, Jiang W, Duan N, Qian Y, Zhou Q, Ye P, Jiang H, Bai Y, Zhang W, Wang W. NOD1, RIP2 and Caspase12 are potentially novel biomarkers for oral squamous cell carcinoma development and progression. *Int J Clin Exp Pathol*. 2014;7(4):1677–1686. PMID: 24817964; PMCID: PMC4014248.
- Warf MB, Berglund JA. Role of RNA structure in regulating pre-mRNA splicing. *Trends Biochem Sci*. 2010;35(3):169–178. <https://doi.org/10.1016/j.tibs.2009.10.004>.
- Weinstein JN, Collisson EA, Mills GB, Shaw KRM, Ozenberger BA, Ellrott K, Shmulevich I, Sander C, Stuart JM. The cancer genome atlas pan-cancer analysis project. *Nat Genet*. 2013;45(10):1113–1120. <https://doi.org/10.1038/ng.2764>.
- Wetsel WC. Hyperthermic effects on behavior. *Int J Hyperthermia*. 2011;27(4):353–373. <https://doi.org/10.3109/02656736.2010.550905>.
- Xing Y, Lee C. Evidence of functional selection pressure for alternative splicing events that accelerate evolution of protein subsequences. *Proc Natl Acad Sci U S A*. 2005;102(38):13526–13531. <https://doi.org/10.1073/pnas.0501213102>.
- Xu F, Li R, von Gromoff ED, Drepper F, Knapp B, Warscheid B, Baumeister R, Qi W. Reprogramming of the transcriptome after heat stress mediates heat hormesis in *Caenorhabditis elegans*. *Nat Commun*. 2023;14(1):4176. <https://doi.org/10.1038/s41467-023-39882-8>.
- Xu C, Zhang J. Mammalian alternative translation initiation is mostly nonadaptive. *Mol Biol Evol*. 2020;37(7):2015–2028. <https://doi.org/10.1093/molbev/msaa063>.
- Yan X, Xiu F, An H, Wang X, Wang J, Cao X. Fever range temperature promotes TLR4 expression and signaling in dendritic cells. *Life Sci*. 2007;80(4):307–313. <https://doi.org/10.1016/j.lfs.2006.09.022>.
- Zare A, Petrova A, Agoumi M, Armstrong H, Bigras G, Tonkin K, Wine E, Baksh S. RIPK2: new elements in modulating inflammatory breast cancer pathogenesis. *Cancers (Basel)*. 2018;10(6):184. <https://doi.org/10.3390/cancers10060184>.
- Zeng Z, Sharpe CR, Simons JP, Gorecki DC. The expression and alternative splicing of alpha-neurexins during *Xenopus* development. *Int J Dev Biol*. 2006;50(1):39–46. <https://doi.org/10.1387/ijdb.052068zz>.
- Zhang H, Ma Y, Zhang Q, Liu R, Luo H, Wang X. A pancancer analysis of the carcinogenic role of receptor-interacting serine/threonine protein kinase-2 (RIPK2) in human tumours. *BMC Med Genomics*. 2022;15(1):97. <https://doi.org/10.1186/s12920-022-01239-3>.
- Zhang Y, Yan L, Zeng J, Zhou H, Liu H, Yu G, Yao W, Chen K, Ye Z, Xu H. Pan-cancer analysis of clinical relevance of alternative splicing events in 31 human cancers. *Oncogene*. 2019;38(40):6678–6695. <https://doi.org/10.1038/s41388-019-0910-7>.
- Zhao W, An H, Zhou J, Xu H, Yu Y, Cao X. Hyperthermia differentially regulates TLR4 and TLR2-mediated innate immune response. *Immunol Lett*. 2007;108(2):137–142. <https://doi.org/10.1016/j.imlet.2006.11.008>.
- Zhou J, Zhang Q, Zhao Y, Song Y, Leng Y, Chen M, Zhou S, Wang Z. The regulatory role of alternative splicing in inflammatory bowel disease. *Front Immunol*. 2023;14:1095267. <https://doi.org/10.3389/fimmu.2023.1095267>.
- Zou C, Zan X, Jia Z, Zheng L, Gu Y, Liu F, Han Y, Xu C, Wu A, Zhi Q. Crosstalk between alternative splicing and inflammatory bowel disease: basic mechanisms, biotechnological progresses and future perspectives. *Clin Transl Med*. 2023;13(11):e1479. <https://doi.org/10.1002/ctm2.1479>.

Associate editor: Esther Betran